THE EFFECTS OF THE NANOTOPOGRAPHY OF TITANIUM SURFACES ON OSTEOBLAST ADHESION AND DIFFERENTIATION

by

PRICILLA SANTIAGO MEDINA

A thesis submitted in partial fulfillment of the requirements for the degree of

MASTER OF SCIENCE
in
BIOLOGY

UNIVERSITY OF PUERTO RICO
MAYAGÜEZ CAMPUS
2013

Approved by:

_____   _____
Vivian Navas Almeyda, Ph.D.   Date
Member, Graduate Committee

_____   _____
Paul A. Sundaram, Ph.D.   Date
Member, Graduate Committee

_____   _____
Monica Alfaro, Ph.D.   Date
Member, Graduate Committee

_____   _____
Nanette Diffoot-Carlo, Ph.D.   Date
President, Graduate Committee

_____   _____
Abner Rodríguez-Carías, Ph.D.   Date
Representative of Graduate Studies

_____   _____
Nanette Diffoot-Carlo, Ph.D.   Date
Chairperson, Biology Department

Abstract

The principal problem in current orthopedic implants is their loosening due to poor osseointegration. Many efforts have been made to modify the surface composition and topography of titanium alloy implants to attain improved osseointegration. A good combination of porous and thick oxide films on titanium alloy substrates have been obtained with the use of the micro arc oxidation (MAO) procedure. This technique incorporates calcium and phosphorus forming calcium phosphate, a chemical commonly applied to metallic implants as a coating material for fast and firm fixation. The first step in determining the biocompatibility of such modified surfaces is to study cell attachment and proliferation on these substrates. Hence, in the work described herein, the adhesion of human osteoblasts to micro arc oxidized Ti-6Al-4V and γ-TiAl surfaces was examined *in vitro*. hFOB 1.19 cells were seeded on micro arc oxidized γ-TiAl (MAOGTi) and Ti-6Al-4V (MAOTiV) disks, respectively. Cell adhesion on γ-TiAl and Ti-6Al-4V thermally oxidized at both 500ºC and 800ºC were also evaluated.

The human fetal osteoblast cell line (hFOB 1.19) consists of immortalized cells that can be subcultured for a long period of time (up to eight months). In addition, they have the ability to differentiate into mature osteoblasts. For comparison purposes, cell morphology and differentiation was observed on thermally oxidized Ti-6Al-4V and γTiAl alloys at 500°C (GTi5, TiV5) and at 800°C (GTi8, TiV8). These alloys were incubated with human fetal osteoblast cell line (hFOB 1.19) at different incubation time points (3 days at 33.5°C and 7 days at 39.5°C) and analyzed by Scanning Electron Microscopy (SEM) and the Alkaline Phosphatase Assay (ALP). Glass coverslips, positive control, were also incubated at these time points. Scanning Electron Microscopy (SEM) and an Alkaline Phosphatase Assay were used to evaluate cell adhesion and cell differentiation on the different surfaces. The Alkaline Phosphatase Assay, at 10 days post seeding, showed significant differences in cell differentiation demonstrating that the roughest surface with treatment and time of exposure of 225mA and 4 minutes was more favorable and Ti-6Al-4V and γ-TiAl alloys without treatment were less favorable, with *p* values < 0.05 between micro arc oxidized and thermally oxidized coated alloys, Ti-6Al-4V and γ-TiAl, respectively. All SEM images showed that cells adhered on all but TiV8 surfaces, 10 days post seeding.

In addition, these highly porous, uniform and thick coatings produced on the surface of both alloys were studied and compared using Atomic Force Microscopy (AFM). A significant

relationship was found between the coating characteristics and the voltage-current conditions applied during the micro arc oxidation process. This demonstrated that the surface exposed to the (225mA and 4 minutes) most amperage and time of exposure was the roughest.

The SEM analysis demonstrated that hFOB 1.19 cells were able to attach and proliferate on both micro arc oxidized and thermally oxidized γ-TiAl surfaces in a similar manner; however, ALP analysis demonstrated that cell differentiation was significantly higher in the γ-TiAl micro arc oxidized alloys in comparison to Ti-6Al-4V alloys.

Resumen

El principal problema en implantes ortopédicos actuales es su aflojamiento debido a pobre oseointegración. Muchos esfuerzos han sido realizados para modificar la composición y la topografía de las superficies de aleaciones de titanio, usados en implantes para alcanzar una mejor oseointegración. Una combinación buena de superficies porosas y gruesas de óxido en sustratos de aleaciones de titanio ha sido obtenida con el uso de la técnica de oxidación micro arco (MAO). Esta técnica integra calcio y fósforo que forman fosfato cálcico, una sustancia química aplicado comúnmente a implantes metálicos para una fijación rápida y firme. El primer paso en determinar la biocompatibilidad de tales superficies modificadas es estudiar la adhesión y proliferación de los osteoblastos en estos sustratos. Por ende, en el trabajo descrito, la adhesión y diferenciación de los osteoblastos humanos en las aleaciones Ti-6Al-4V y γ-TiAl oxidados por la técnica de micro arco se evaluaron *in vitro*. Las células hFOB 1.19 fueron sembradas en los discos de las aleaciones de Ti-6Al-4V (MAOTiV) y γ-TiAl oxidados por la técnica de micro arco (MAOGTi), respectivamente. También, la adhesión de estas células fue evaluada en las aleaciones de γ-TiAl y Ti-6Al-4V oxidados térmicamente a 500ºC y 800ºC. La línea fetal humana de osteoblastos (hFOB 1,19) consiste en células inmortalizadas que pueden ser sub-cultivadas por un periodo de tiempo largo (hasta ocho meses). Además, tienen la capacidad de diferenciarse a osteoblastos maduros. Para propósitos de comparación, la morfología y diferenciación de las células fueron observadas en las aleaciones Ti-6Al-4V y γ-TiAl térmicamente oxidados a 500°C (GTi5, TiV5) y 800°C (GTi8, TiV8). Estas aleaciones fueron incubadas con la línea fetal humana de osteoblastos (hFOB 1,19) en puntos diferentes de tiempo de incubación (3 días en 33.5°C y 7 días en 39.5° C) y analizadas mediante la Microscopia Electrónica de Rastreo (SEM) y el Ensayo Colorimétrico de Fosfatasa Alcalina (ALP). Cubreobjetos de vidrio, el control positivo, también fueron incubados en estos puntos de tiempo. La Microscopia Electrónica de Rastreo (SEM) y el Ensayo de Fosfatasa Alcalina fueron utilizados para evaluar adhesión y diferenciación de las células en las diferentes superficies. El Ensayo de Fosfatasa Alcalina, después de 10 días de incubación, demostró diferencias significativas en la superficie más áspera con tratamiento y tiempo de exposición de 225mA y 4 minutos. Este fue más favorable, con valores P <0,05 entre las aleaciones Ti-6Al-4V y γ-TiAl oxidados por la técnica de micro arco y térmicamente oxidado, respectivamente. Todas las

imágenes de SEM mostraron que las células se adhirieron en todas las superficies menos en TiV8, luego de 10 días de incubación.

Además, estas capas sumamente porosas, uniformes y gruesas producidas en la superficie de ambas aleaciones fueron estudiadas y fueron comparadas utilizando la Microscopia de Fuerza Atómica (AFM). Una relación significativa fue encontrada entre las características de capa y las condiciones de voltaje-corriente aplicadas durante el proceso de oxidación por la técnica de micro arco. Esto demostró que la aleación de Ti-6Al-4V tratada por la técnica de micro arco (225mA y 4 minutos) fue el más áspero. El análisis de SEM demostró que las células hFOB 1.19 pudieron adherirse y proliferarse en ambas superficies tratadas por la técnica de micro arco y térmicamente oxidada en una manera semejante; sin embargo, el análisis de ALP demostró que la diferenciación de las células fue más alta en las aleaciones de γ-TiAl oxidadas con la técnica de micro arco con respecto a las aleaciones de Ti-6Al-4V.

Dedication

This thesis is dedicated to my husband Jonathan Barbosa, my daughter Yaslee Johanelys and my son Nolan Zahir, for the love that they give me every day. This is for my husband for his patience and support during the completion of this work; for my daughter for the beautiful smile that she gave me every day when I got back home and for my son for giving me more motivation to complete this work. They are my force and the reason that I have to try to be a better person every day of my life.

Table of Contents

List of Tables

List of Figures

Figure 24: Morphological characterization of micro oxidized Ti-6Al-4V and γ-TiAl alloys by AFM. Each column shows the surface appearance by Atomic Force Microscopy at each treatment (without treatment, 500°C, 800°C, 200mA at 3 and 4 minutes, and 225mA at 3 min and 4 minutes of treatment) respectively. Average roughness (a.r) is represented in nanometers

1. Introduction

Titanium (Ti) and its alloys have been used as implant materials due to their excellent biocompatibility [11]. Ti-6Al-4V is the most common titanium alloy used in bone repair and replacement. However, the possibility of vanadium release from Ti–6Al–4V and its poor shear strength, which can cause a high coefficient of friction, in both bone-metal and metal-metal interfaces, have broadened the search for other materials [11]. Also, it has been frequently reported that titanium oxide debris is formed in Ti implants causing immunological reactions that result in loosening of the implants at the metal-bone interface [4]. This has led to the study of Ti alloys without vanadium and with mechanical properties comparable to those of Ti–6Al–4V as possible implant materials. New materials are being proposed for use in implants with superior biocompatibility properties than those of commercially pure (cp Ti) and Ti-6Al-4V alloys [11]. The Ti alloy, γ titanium aluminide (γ-TiAl), has excellent properties compared to those of Ti-6Al-4V, with possible biological implant applications. γ-TiAl alloys have low density (3.8 g/cm^3), high stiffness and mechanical strength (up to 1000 MPa) [40], and good oxidation and corrosion properties [65]. This titanium alloy has superior corrosion resistance, high specific strength and rigidity, and lower density than currently used Ti alloys. γ-TiAl implants can form aluminum oxide instead of titanium oxide when heated to appropriate temperatures, which will resist wear and loss of particles, thus avoiding the negative response of the immune system, and therefore these appear to have properties suitable for implant material.

New titanium alloy compositions have been developed to further enhance osseointegration. For promoting and accomplishing osseointegration, a surface modification involving a thermodynamically stable oxide film naturally formed on the surface is regarded as the most determining factor for mechanical bonding with bone tissue [2,67,75].

Titanium and its alloys spontaneously form a thin biocompatible surface oxide layer, composed primarily of TiO_2. When the titanium alloy is implanted *in vivo*, the oxide stability may be altered resulting in increased metal ion release and implant failure [61]. Several treatments have been developed to modify the surface oxides on Ti alloys to improve wear resistance. Advanced surface modification methods (e.g. plasma ion implantation), anodizing, ultrapassivation, nitriding, electrochemical and thermal oxidation has been applied to Ti-6Al-4V leading to the formation of stable superficial oxides [2,11,15,38]. Among the methods used to modify the properties of the oxide layer, the micro arc oxidation (MAO) procedure has been

reported to be a preferred method to provide a good combination of porous and thick oxide films with a well characterized biocompatible substrate containing Ca and P. The TiO_2 layer generated by the MAO treatment was found to significantly improve the cellular activities of titanium alloys *in vitro* and the bone-implant bonding properties *in vivo* [45]. These improvements were attributed to an increase in the surface roughness, as well as to the incorporation of Ca and P into the coating layer. The porous and rough morphology produced by the MAO process increased cell attachment and mechanical interlocking between the tissue and implant. Moreover, the Ca and P source, incorporated from the electrolyte in the oxide layer, improved the osteoblast cell response and enhanced osseointegration [75].

To achieve enhanced osseointegration, an electrochemical surface treatment (micro arc oxidation) was proposed in this study. The oxide coatings were generated on Ti-6Al-4V and γ-TiAl alloys. Human fetal osteoblast cells (hFOB1.19) were seeded on these oxide coatings to study cell adhesion and differentiation. This novel oxide coating could result in the generation of implants that result in the formation of a characteristic interfacial layer with adequate biomechanical properties, also providing insight of the events that occur at the bone–material interface.

Micro arc oxidation (MAO) also enhances corrosion resistance and bioactivity as a result of the formation of a thicker oxide coating and the inclusion of calcium and phosphorous ions in this coating [41]. Corrosion is a deteriorating reaction that occurs in metallic materials when they come in contact with an environment of body fluids. Corrosion may lead to undesirable release of metal ions, which potentially may have localized or systemic cytotoxic, genotoxic and even carcinogenic effects *in vivo* [79]. Therefore, micro arc oxidation is considered to be one of the most useful methods for surface modifications because it produces porous and firmly adherent TiO_2 films on Ti implants [2]. These properties enhance the fixation of the implants to the bone and improve their *in vivo* corrosion behavior. This technique makes full use of the anodic oxidation of Ti alloys by applying a positive voltage to a Ti substrate used as the anode immersed in an electrolyte. When an applied voltage is increased beyond a certain point, micro arcs are generated as a result of the dielectric breakdown of the surface TiO_2 layer, where Ti ions in the Ti implant and OH ions in the electrolyte move in opposite directions very quickly to form TiO_2 again. In addition, the use of an electrolyte solution containing Ca and P ions results in improved osseointegration properties in *in vivo* tests since Ca and P are incorporated into the

oxide layer formed during the MAO process. Different from anodic oxidation, MAO has specific characteristics, such as producing local high temperatures, and forming a ceramic coating. The type of electrolyte used and electric conditions applied can affect the surface morphology, chemical composition, and crystalline structure of the oxide coatings formed by MAO.

The main objective of this research was to study and compare *in vitro* cell adhesion and differentiation of human fetal osteoblast cells hFOB 1.19 cultured on micro arc and thermally oxidized γ-TiAl and Ti-6Al-4V with different nanotopographies resulting from the oxidation processes. The human fetal osteoblast cell line (hFOB 1.19), was used to evaluate cell adhesion and differentiation on thermally and micro arc oxidized Ti-6Al-4V and γ-TiAl alloys. This cell line is isolated from fetal tissue and transfected with a gene coding for a temperature-sensitive (tsA58) mutant and a gene coding for neomycin (G418) resistance. Incubation of hFOB cells at the permissive temperature (33.5°C) results in rapid cell division, whereas at a restrictive temperature (39.5°C), they have the ability to differentiate into mature osteoblasts.

Cell differentiation was detected using the Alkaline Phosphatase Assay. Alkaline phosphatase (ALP) is the most widely recognized biochemical marker for osteoblast activity and plays a role in skeletal mineralization. Cell attachment was qualitatively observed using Scanning Electron Microscopy (SEM). This technique provides information about cell attachment and proliferation. Thermally oxidized Ti-6Al–4V and γ-TiAl were used to compare the results obtained with the micro arc oxidized alloys. Thus, to determine cytocompatibility and osseointegration a combination of assays are necessary to measure the various stages of cell-material interaction.

In summary, previous studies have established that micro arc oxidation of γ- TiAl and Ti-6Al-4V increases cell attachment and cell differentiation as well as the corrosion resistance and antibacterial efficacy of the Ti alloys [5]. Thus, it is expected that the micro arc oxidized titanium surfaces would exhibit similar or better biocompatibility properties compared to thermally oxidized γ-TiAl and Ti-6Al-4V surfaces. Depending on the micro arc oxidation conditions, different roughness of titanium oxides are formed on Ti alloys; thus, it is expected that osteoblast cells respond differently to surface oxides formed on micro arc oxidized surfaces in comparison to thermally oxidized surfaces.

2. Literature Review

In biomaterial science, biocompatibility refers to the behavior of a material in environments of variable bio-chemical and bio-physical conditions [15]. The term may refer to specific properties of a material without specifying where or how the material is to be used. These properties determine the clinical success of any medical device developed such as a heart valve or that which is used for bone repair or replacement. Metals currently used in bone repair and replacement include stainless steel, Cr-Co alloys and commercially pure (cp) titanium and its alloys. However, the use of these alloys have presented some disadvantages such as the dissociation of the implant from the bone after a ten year period and the significant pain in the amputee, reason for exploring materials with direct bone attachment (better known as osseointegration).

2.1 Composition of bone

Bone is a hard vascular connective tissue that consists of cells and an extracellular matrix. It is composed of hydroxyapatite ($Ca_{10}(PO_4)_6(OH)_2$) crystals deposited within an organic matrix (95% is Type I collagen) [35,48,61]. The morphology consists of trabecular bone which creates a porous environment (50–90% porosity) and pore sizes of 1 mm diameter [34], with surrounding cortical bone. As seen in Figure 1, long bone has a dense and rigid outer shell of compact bone called the cortex, and a cancellous or spongy zone of thin interconnecting narrow bone trabeculae (central medullary) [30,34,36,61,64,80].
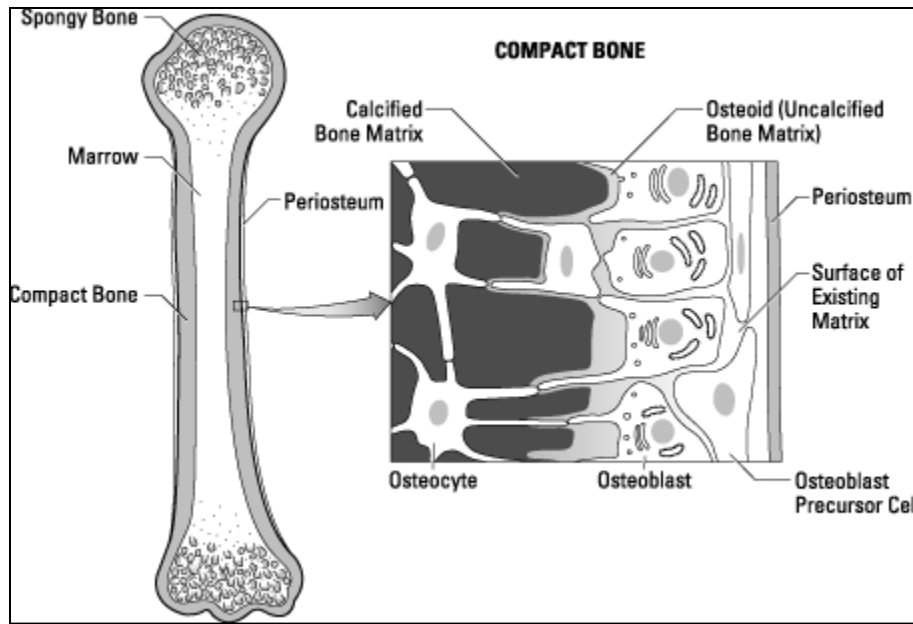
Figure 1: Bone Internal and External structures [30].

The cellular component of bone consists of three types of cells: osteoclasts, osteoblasts and osteocytes [61,63,80]. Osteoclasts are large multinuclear cells derived from monocytes which are important in bone remodeling and which can be found on the surface of the bone. Osteoblasts are cuboidal cells found on the surface of new bone where they synthesize the bone matrix. As osteoblasts make the bone matrix, they become trapped as the matrix calcifies, and these trapped osteoblasts are known as osteocytes. Osteocytes are flattened, discoid cells found inside the bone and are responsible for bone maintenance. They can sense pressure or cracks within the bone, directing osteoclasts to dissolve the bone as and when necessary. Osteoblasts and osteoclasts are responsible for the formation, remodeling and repair of the bone. They are also responsible for the osseointegration of nanostructured biomaterials in orthopedics [70].

Bone differs from other connective tissue in the mineralization of the extracellular matrix. The extracellular matrix of bone is composed of 90% collagenic proteins (Type I collagen and Type V collagen) and 10% non-collagenic proteins (osteocalcin, osteonectin, bone sialoproteins, proteoglycans, etc.). All these proteins are synthesized by osteoblasts and most of these proteins are involved in cell adhesion. The extracellular matrix has a variety of functions such as support, protection and homeostasis [2,34-35,61,78].

The cellular component of the bone consists of different cells. Osteoprogenitor cells are derived from mesenchymal stem cells, which give rise to osteoblasts [80]. These cells are found on the bone surface that lay down the extracellular matrix and regulate bone mineralization.

These mononuclear cells are also responsible for osteoid calcification. The calcification process is initiated when the osteoblasts secrete the matrix vesicles which are rich in alkaline phosphatase [34]. Osteoblasts are large cells with abundant basophilic cytoplasm, a prominent Golgi apparatus and are potent to produce osteoid, a collagen I rich matrix [6]. These cells are anchorage dependent and rely on cell-matrix and cell-cell contacts via a variety of transmembranous proteins (integrins, cadherins, connexins) and specific receptors (cytokines, hormones, growth factors) to maintain cellular function and responsiveness to metabolic and mechanical stimuli.

2.2 Human Osteoblastic cell culture

Different osteoblastic cell lines have been used to determine cell adhesion on biomaterials *in vitro*. The most widely used osteoblastic cells include primary cultures derived from human or rodent tissue, as well as osteosarcoma cell lines derived from human and rodent tumors [9]. However, these osteoblastic cells have limitations with regard to their application to the study of human osteoblast biology *in vitro*. Osteoblastic cultures derived from rodent species may exhibit species-specific phenotypic characteristics which differ from those of human osteoblastic cultures. Osteosarcoma cell lines have an inherent uncertainty with regard to their phenotypic similarity to untransformed cells. Primary cultures derived from normal human bone have an osteoblastic phenotype but proliferate at a very slow rate. Since hFOB 1.19 cells have the ability to differentiate into mature osteoblasts and can be subcultured for a long period of time due to their immortality, they constitute a valuable option in research related to bone replacing materials [6,61]. This cell line has been used to study the effects of the surface characteristics of different substrata on osteoblast phenotypic responses [6,61,78].

The human osteoblast cell line (hFOB 1.19) was obtained from a primary culture of fetal tissue and transfected with a gene that codes for a temperature-sensitive mutant (tsA58) of the SV40 large T antigen and a gene encoding for neomycin (G418) resistance [29]. Incubation of hFOB cells at the permissive temperature (33.5°C) results in a rapid cell division, whereas little or no cell division occurs at the restrictive temperature (39.5°C). The cell line hFOB 1.19 can be cultured at 33.5°C for up to passage 30 without problems, thereafter which (at passage 32-34) proliferation slows considerably [29]. Post-confluent hFOB cells cultured at 33.5°C demonstrate high levels of osteopontin (OP), osteonectin (ON), bone sialoprotein (BSP) and collagen type I

[20]. Furthermore, the cell line hFOB exhibits an increase of cAMP levels in response to 1-34 parathyroid hormone (PTH) treatment, an increase of osteocalcin and alkaline phosphatase activity in response to dihydroxyvitamin D3 treatment (1, 25 D3) and formation of mineralized nodules [29].

2.3 Biomaterials

A biomaterial is a nonviable material used in a medical device, intended to interact with a biological system [59]. These biomaterials are used to repair, assist or replace living tissue or organs that are functioning below an acceptable physiological level. Biocompatibility is the ability of a material to perform with an appropriate host action for a specific application [59]. The most important characteristics required of implant metals are adequate levels of biocompatibility, strength, and corrosion resistance [61].

Common degradable and non-degradable implant materials can be divided into synthetically produced metals and metal alloys, ceramics, polymers, and composites or modified natural material [59]. Whereas non-absorbable materials, like steel or titanium alloys, are commonly used for prosthetic devices, resorbable bone substitute materials are mainly studied for their feasibility in bone replacement therapies. Various approaches used in the design of bone substitute materials have focused on the degradation and ultimate replacement of the material with new tissue. Irrespective of a material being biodegradable or not, its surface properties will influence the initial cellular events at the cell-material interface. The   degree of degradation of the surface of the biomaterial influences greatly the proliferation of osteoblasts and therefore its response will depend on the stage of degradation. The cellular response of osteoblasts to the material surface needs to be considered in order to engineer or design a optimal implant for biomedical applications.

Four types of materials have been experimentally and/or clinically studied as bone substitute materials or scaffold materials for applications in tissue engineering. These include biodegradable and bioresorbable polymers (polyglycolide, polydioxanone, and polycaprolactone), polymers which are under current clinical investigation (polyorthoester, polyanhydrides, and polyhydro-xyalkanoate) and entrepreneurial polymeric biomaterials (poly (lactic acid-co-lysine). There has also, been the use of synthetic inorganic materials

(hydroxyapatite, calcium/phosphate composites, glass ceramics), organic materials of natural origin (collagen, fibrin, hyaluronic acid) and inorganic materials of natural origin (coralline hydroxyapatite) as biomaterials [6].

In the metallic biomaterials, titanium and its alloys have gained more attention as biomaterials due to their lower modulus, superior biocompatibility, and enhanced corrosion resistance when compared to more conventional stainless steels and cobalt-based alloys [61]. Titanium is a low density element that can be highly strengthened by an alloying and deformation process.

Titanium is located in group 4, position 22 of the periodic table. This group lies in the d-block of the periodic table. The group itself has not acquired a trivial name; it belongs to the broader grouping of the transition metals. A transition metal is defined as an element whose atom has an incomplete *d* sub-shell, or which can give rise to cations with an incomplete *d* sub-shell. The physical properties that put titanium in the group 4 elements are that it has a melting point of 1941 K (1668°C), a boiling point of 3560 K (3287°C), a density 4.507 g cm, is of a silver metallic appearance and has an atomic radius of 140 pm [Figure 2] .

Figure 2: Periodic Table of Elements [58]. The black circle denotes the localization of the element titanium.

Titanium and its alloys used for implant devices have been designed to have excellent biocompatibility, with little or no reaction with tissue surrounding the implant. Titanium derives its corrosion resistance from the stable oxide film that forms on its surface, which can reform if damaged at body temperatures and in physiological fluids [6].

Ti-6Al-4V is the most commonly used titanium alloy. It contains 6% Aluminum and 4% Vanadium. This alloy exhibits an excellent combination of corrosion resistance, strength, low modulus of elasticity, and toughness, but it suffers from low fracture toughness and poor wear properties [6]. Its excellent corrosion resistance is due to the formation of a solid oxide film on the surface that passivates the material [23]. Titanium alloys have a strong affinity for oxygen, thus promoting the formation of a stable and tightly adherent protective oxide layer on their surface. Since this oxide layer is in direct contact with biological tissue, the chemical composition and stability of this surface oxide layer is important and will affect implant success. Some disadvantages of titanium alloys are their low fracture toughness, poor wear properties and high coefficient of friction. Furthermore, their clinical use has raised some concerns due to problems caused by the release of vanadium (V) from Ti-6Al-4V alloys. Vanadium has been reported to be toxic and shows adverse tissue effects [6]. Consequently, new titanium alloy compositions are being developed. Among these are the γ titanium aluminide alloys [6].

γ-titanium aluminide (γ-TiAl) is an intermetallic material commonly used in applications where high temperature is required (aerospace and automotive applications) [61]. This alloy has excellent properties compared to Ti-6Al-4V. γ-TiAl offers superior corrosion resistance, high specific strength and rigidity, and a lower density compared to Ti-6Al-4V [19]. In addition, this material is proposed to possess excellent biocompatibility and good long-term fatigue and wear properties. These characteristics make γ-TiAl very attractive for high temperature applications in aggressive environments as well as for endoprothestic applications. The use of γ-TiAl as a substitute for Ti-6Al-4V will eliminate the possible presence of vanadium, thus reducing its possible effects in the bone-implant interface [61]. Preliminary studies were performed using γ-TiAl implants in *in vivo* models in rats with cell attachment and bone tissue formation demonstrating a favorable tissue response and its potential to be used as implant material [69]. A study evaluating the corrosion resistance of γ-TiAl in a body fluid environment shows similar corrosion resistance similar toTi-6Al-4V [8,17].

All biomaterials possess a complex three dimensional surface topography consisting of regular or non-regular micrometer and nanometer sized features. Barthlott *et al.,* [5] demonstrated that surface properties are related both to molecular interactions and the surface topography. Therefore, the difference in surface properties may have profound effects on the protein adhesion and the resulting cellular attachment.

2.4 Osteoblast adhesion to biomaterials

Orthopedic and dental implants are said to osseointegrate if a solid interface is obtained between the material surface and the bone tissue with no intermediate soft tissue formation [6]. Osseointegration depends highly on the material's biocompatibility and this property is related to cell behavior when in contact with the biomaterial. The term "adhesion" in the biomaterial domain covers two different phenomena: the attachment and adhesion phases [2]. The attachment phase occurs rapidly and involves short-term events like physicochemical linkages between cells and materials involving ionic forces and van der Waals forces. The adhesion phase occurs over longer periods of time and involves various biological molecules (extracellular matrix proteins, cell membrane proteins, and cytoskeleton proteins) which interact together to induce the subsequent cell response with respect to migration and differentiation. Davis *et al.,* [16] determined that a bone-like mineral formation at the material surface should be the ultimate stage of a bonelike osteoblast reaction. The outcome of the long term osteoblast reaction is further influenced by the biophysical (mechanical and electrical) environment which will be present at the material/cell interface under functional conditions.

Cells that express integrins (cell membrane receptors) are able to adhere to implant surfaces covered with extracellular proteins originated from blood or serum. Some of the bone proteins have chemotactic or adhesive properties, notably because they contain an Arg-Gly-Asp (RGD) sequence which is specific to the fixation of cell membrane receptors (integrins) [2]. The sites of adhesion between tissue cultured cells and substrate surfaces are called focal contacts or adhesion plaques. Focal contacts are closed junctions where the distance between the substrate surface and the cell membrane is between 10 and 15 nm. The formation of focal contacts is promoted *in vitro* by extracellular matrix proteins (fibronectin, vitronectin) [20].

Adhesion molecules are characterized by their capacity to interact with a specific ligand. These ligands may be present on the membrane of neighboring cells or on extracellular matrix

proteins. The four main classes of adhesion molecules are selectins, immunoglobulins, cadherins and integrins. Amongst them, only cadherins and integrins have been described for osteoblastic cells. Selectins are heterophilic molecules that bind fucosylated carbohydrates, immunoglobulins are proteins that are used by the immune system to neutralize bacteria or viruses. Cadherins are homophilic calcium dependant glycoproteins and integrins are one of the major classes of receptors within the extracellular matrix [7].

Integrins are transmembrane heterodimers consisting of noncovalently associated α and β subunits. Each subunit is made up of a large extracellular domain, a transmembrane domain and a short cytoplasmic domain. The integrin across the cell membrane acts as an interface between the intracellular and extracellular compartments and can translate the attachment of external ligands to internal information which induces adhesion, spreading, or cell migration and consequently regulates cell growth and differentiation [7] [Figure 3].
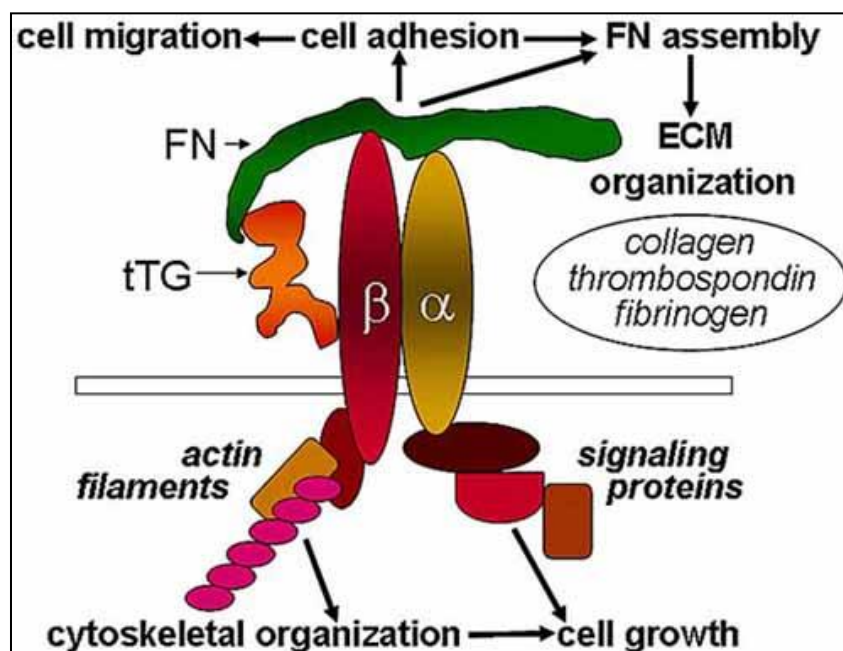
Figure 3: Integrin Structure. Source: Frontiers in Bioscience [31].

2.5 Nanotopography to enhance osseointegration

Nanobiomaterials are characterized by constituent particles and/or surface features less than 100nm in at least one dimension [71]. Nanolayers are used to enhance the surface biocompatibility of drug delivery systems, control the release of substances such as antibiotics or growth factors, act as gene-delivery vehicles, or serve as light emitters for cellular labeling and tracking [33]. Nanotechnology is also applied to modify and improve the surface structure in

orthopedic implants to promote osseointegration. However, there are side-effects from the use of nano particles *in vivo*. The use of nano particles can induce or promote inflammatory reactions and also influence blood coagulation [14,25,42,73]. Therefore, the cytocompatibility of a biomaterial is strongly influenced by its chemical composition. Furthermore, surface topography plays a crucial role for cell-surface interactions.

Cell-surface interactions play a crucial role for biomaterial application in orthopedics. It is evident that not only the chemical composition of solid substances influences cellular properties (adherence, migration, proliferation and differentiation) but also the surface topography of a biomaterial. The progressive application of nanostructured surfaces in medicine has generated interest to improve the cytocompatibility and osseointegration of orthopedic implants. A nanostructured surface (scaffold) is a three dimensional substrate that serves as a template for tissue regeneration. The ideal scaffold should have an appropriate surface chemistry and microstructure to facilitate cellular attachment, proliferation and differentiation. In addition, the scaffold should have an adequate mechanical strength and biodegradation rate without any undesirable by-products [68].

These scaffolds could serve as a synthetic extracellular matrix (ECM) to organize cells into a three-dimensional (3D) architecture and to present stimuli, which direct the growth and formation of a desired tissue [74]. Ideally, the scaffold acting as an artificial extracellular matrix (ECM) should perform the structural and biochemical functions of the ECM until the cell-produces its own ECM.

However, most scaffolds do not take biology into consideration and thus have limited efficacy. Perhaps one of the greatest challenges faced in tissue engineered devices, regardless of tissue type, is allowing blood-vessel formation (angiogenesis) and promoting healing in three dimensions which is critical to the success of the scaffold. Therefore, various methods have been developed to modify the degree of roughness as well as surface energy and topography in orthopedic implants. Typically applied techniques to enhance the degree of roughness and promote the osseointegrative properties of metallic biomaterials are chemical etching, anodization, sand-blasting, sputtercoating, and machine-tooling.

It has been shown that nanoparticle surfaces created by anodization have promoted osteoblast adhesion up to three times greater compared to unanodized Ti [73]. Ward *et al.,*[73, 74] demonstrated that the initial attachment of osteoblasts onto the surface of metals such as

cpTi, Ti-6Al-4V, and CoCrMo is enhanced by the addition of submicron to nanometer particles compared to metals composed of micron particles. One possible explanation of this phenomenon is the greater amount of particle binding sites for osteoblast adhesion at the surfaces of nanophase metals in comparison to micron particle size metals. The theory of enhanced protein and cell binding capacities by larger surface areas or roughness was also confirmed for porous hydroxyapatite materials [37].

Once the osteoblasts attach to the material surface, cell migration and proliferation follow. Studies suggest that cells use the nanotopography of a substrate for orientation and migration, responses that should be considered in the design of nanostructured implants [14,43]. Although it is known that bone cells align along defined substrate morphologies (contact guidance), the detailed relation between ordered nanotopography and cell behavior remains unknown [14]. For the first time, in 1964 it was shown that convex surfaces enhance cellular overlap, while grooves minimize cellular overlap [13]. As pre-requisite to reach cell colonization during directed tissue formation, structured nanophase surfaces must lead to a predictable osteoblast orientation and migration on these surfaces.

Focal contacts are important structures for cellular adherence onto a surface but these may delay migration and mobility of the cells. Anselme *et al.,* [2] demonstrated that MG63 cells responded to a nanoscale roughness by having a higher cell thickness and a delayed appearance of focal contacts. In detail, nanoporous Ti-oxide surfaces promoted cellular spreading and induced numerous filopods and osteoblastic differentiation [12,46]. Muller *et al.,* [51] demonstrated the ability of osteoblasts to grow into an open-porous Ti implant and Li *et al.,* [44] also demonstrated that MC3T3-E1 cells attached and were able to divide well in the inner surface of a highly porous Ti-6Al-4V implant. Some *in vitro* studies demonstrated an enhanced total protein and collagen production as well as increased ALP activity of osteoblasts cultured on nanoparticulate metals (cpTi, Ti-6Al-4V, and CoCrMo) indicating advantages of nanostructured surfaces for osseointegration [70,76].

Nanotextured Ti surfaces prepared by chemical etching have upregulated the expression of BSP and OP [14]. Qu *et al.,* [60] demonstrated that the expression of ALP, OC, Type-I-collagen, osteoprotegerin, and glyceraldehyde-3-phosphate-dehydrogenase was promoted by porous Ti surfaces. Ward *et al.,* [73] concluded that nanophase metals induce significantly greater calcium and phosphorus deposition by osteoblasts as well as calcium and phosphorous

precipitation from the culture media in the absence of the osteoblasts. These results were in contrast to microphase Ti-6Al-4V and CoCrMo that was studied by O'Connor *et al.,* [53]. He and his colleagues demonstrated the importance of particle size as a critical factor in osteoblast proliferation and viability *in vitro*.

Numerous variables influence the biocompatibility and osteogenic potency of nanostructured biomaterials *in vitro* and *in vivo*. The surface structure and the composition of a biomaterial affect cellular attachment, adherence, proliferation and migration, and also differentiation and survival of defined cell types. Typical parameters such as chemical composition, surface structure (topography, geometry, roughness and particle size), surface energy, hydrophobicity, and the degree of solubility in aqueous solutions of a biomaterial will help to value and grade a defined implant, concerning its osteoblast promoting potency. Considering recent publications [1,22,28,37,39,52,55,70], it can be expected that wettability of a nanosurface influences protein adsorption significantly, which is a prerequisite for cellular adherence in serum containing solutions. Therefore, nanostructured surfaces enhance the surface area of biomaterials and promote cellular adherence.

2.6 Effects of micro arc oxidation on titanium alloys for osteoblast adhesion

Titanium and its alloys are used in implants due to their excellent biocompatibility with human tissues and mechanical properties. These biocompatibility properties are due to the reactive oxide layer, 4-6nm thick, which forms spontaneously on its surface at room temperature by the reaction of titanium with oxygen. However, Ti-based implant materials do have specific complications such as loosening of the implanted host interface as a result of unsatisfactory cell adhesion and the susceptibility of the implants to bacterial infections. Ti alloys possess no antibacterial activity; therefore a potential risk of plaque formation on Ti implants exists. The accumulation of bacteria on implants causes peri-implantitis that may lead to implant failure. Therefore, new techniques have been developed to prevent bacterial colonization on the surfaces of implants to ensure their long-term clinical success. Most studies have shown that surface modification of oral and transcutaneous implants prevent colonization of bacteria [5]. An effective method to minimize peri-implantitis resulting from bacterial infections on implant surfaces is to modify the surface of the biomaterial.

The presence of the oxide layer on Ti alloys plays an important role in biocompatibility and chemical properties. However, the naturally formed Ti oxide coating is not effective in improving the biocompatibility of a Ti implant due to its limited thickness and poor corrosion resistance. Therefore, oxide coatings on Ti alloys need to be formed using various techniques such as thermal annealing, anodic oxidation and micro arc oxidation (MAO). Among these surface modification techniques, MAO is considered to be one of the most useful methods for surface modifications because it produces porous and firmly adherent TiO_2 films on Ti implants [32]. These properties enhance the fixation of the implants to the bone and improve their *in vivo* corrosion behavior. This technique makes full use of the anodic oxidation of Ti alloys by applying a positive voltage to a Ti substrate used as the anode immersed in an electrolyte. When an applied voltage is increased beyond a certain point, micro arcs are generated as a result of the dielectric breakdown of the surface TiO_2 layer, Ti ions in the Ti implant and OH ions in the electrolyte move in opposite directions very quickly to form TiO_2. In addition, the use of an electrolyte solution containing Ca and P ions resulted in an improvement of the osseointegration properties in *in vivo* tests [69]. Unlike anodic oxidation, MAO has specific characteristics, such as producing local high temperature and the formation of a ceramic coating. The type of electrolyte used and the electric conditions applied can affect the surface morphology, chemical composition, and crystalline structure of the oxide coatings formed by MAO. Among all these parameters, the composition of an electrolyte is the most important factor because of the incorporation of electrolyte elements into the anodic substrate during the oxidation [65].
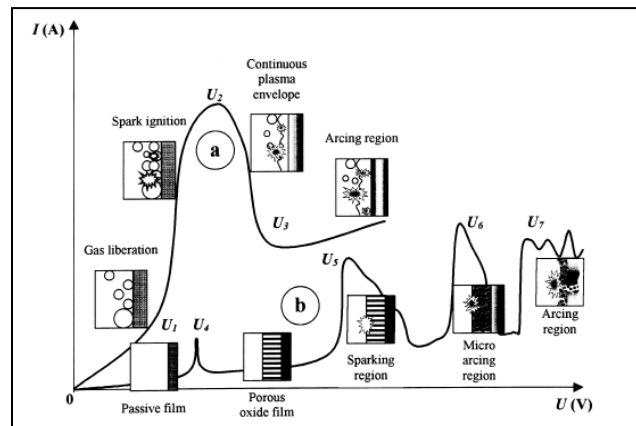
Figure 4: A current–voltage diagram for the micro arc electrolysis: discharge phenomena are developed (a) in the near-electrode area and (b) in the dielectric film on the electrode surface [73].

15

Figure 4 describes the behavior of **a** and **b** type systems. The **b** type system corresponds to micro arc oxidation. The passive film previously formed begins to dissolve at point $U4$, which corresponds to the corrosion potential of the material. In the region of repassivation $U4$–$U5$ a porous oxide film forms, causing a decrease in voltage. At $U5$, the electric field in the electrolyte reaches a critical value beyond which the film is broken due to impact or tunneling ionization. Subsequently, small luminescent sparks move rapidly across the surface of the oxide film promoting its growth. At $U6$, impact ionization is supported by the onset of thermal ionization. This causes the formation of slower, larger arc regions. In the region $U6$–$U7$ thermal ionization is partially blocked by negative charge buildup due to the thickening of the oxide film. This effect determines the relatively low power and duration of the resultant arc discharges, therefore termed as 'micro arcs' [77]. Due to this 'micro-arcing', the film is gradually fused with elements contained in the electrolyte. Beyond the point $U7$, the micro arc discharges occurring throughout the film penetrate through to the substrate and transform into powerful arcs that can translate into thermal cracking of the film.

An electrolyte is defined as any substance containing free ions that make the substance electrically conductive. The electrolyte will conduct electricity when a voltage is applied and electrodes are placed in an electrolyte. Under normal circumstances, lone electrons cannot pass through the electrolyte. A chemical reaction occurs at the cathode where electrons are consumed from the anode. Simultaneously, another reaction occurs at the anode, the electrons produced by this reaction are eventually transferred to the cathode. As a result, a negative charge develops around the cathode in the electrolyte, and a positive charge around the anode. These charges are neutralized by the ions in the electrolyte, enabling the electrons to keep flowing and the reactions to continue. This will facilitate the incorporation of ions in the titanium oxide generated. The ions of interest are calcium and phosphate since it has been demonstrated that bone tissue ingrowth into porous coatings, formed through processes such as MAO, can be further enhanced by the deposition of these ions into the pore walls [71].

Na_2-EDTA molecule is composed of $Na_2.H_2Y$ with $Y= [2(OOC)NCH_2CH_2N(COO)_2]^{4-}$ as graphically depicted in Figure 5.
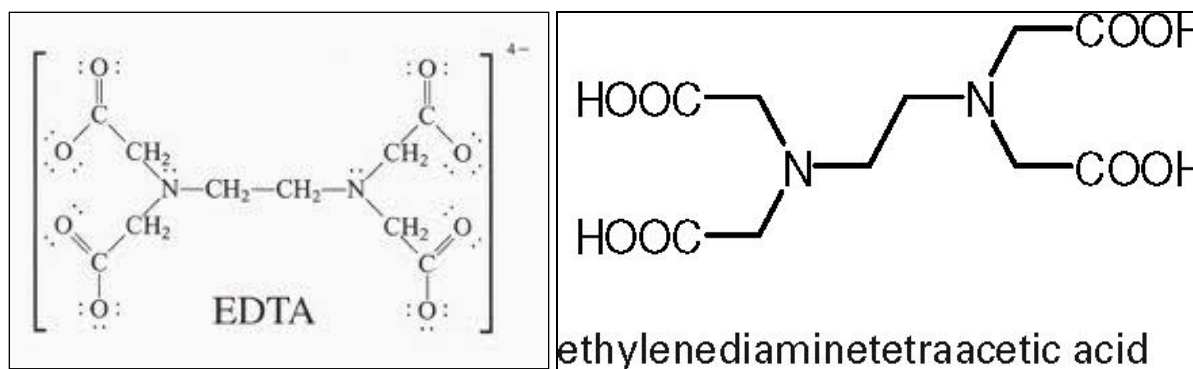
Figure 5: EDTA structure during complex formation [27].

The method of anodizing surface treatment has already been used industrially for treating titanium or aluminum of aircraft parts in Soviet Union. Metals such as titanium can form an oxidation layer if added in a low concentration alkali solution, containing calcium and phosphate. Subsequently, the surface of the metal is oxidized by applying high-voltage and inducing an electric arc. Once the surface of titanium is oxidized through this method, a titanium oxide (TiO_2) layer, which is ceramic, is formed on the surface [Figure 6 and 7]. This surface layer is known to have a very strong bonding strength (80 – 90% of the body) [10, 45,75]. In addition, depending on the added electric pressure level, application method and type of electrolyte, the surface demonstrates a different appearance.
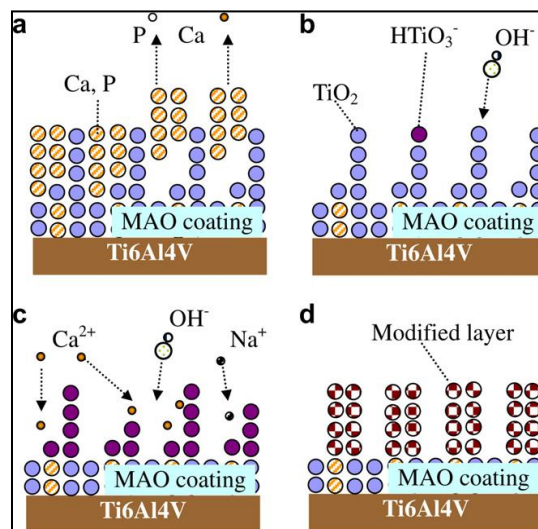
Figure 6: Schematic diagram of the Micro Arc Oxidation coating: (a) the dissolution of Ca and P; (b) the formation of the negatively charged HTiO3 ; (c) the re-deposition of Ca2+ ions, as well as the incorporation of Na+ ions; and (d) the formation of the modified layer [44].

Composition components of the surface commonly consist of calcium and phosphate, and contain a micro porous structure [27,38,41-42,47,57,66,76]. This special structure facilitates osseointegration. Despite the chemical advantages, it is rarely used in the orthopedic field. However in dental implants, in which the initial bone stability is crucial, outstanding results have been reported in comparison to other pre-existing surface treatment methods by the clinical application continued by active research [43].
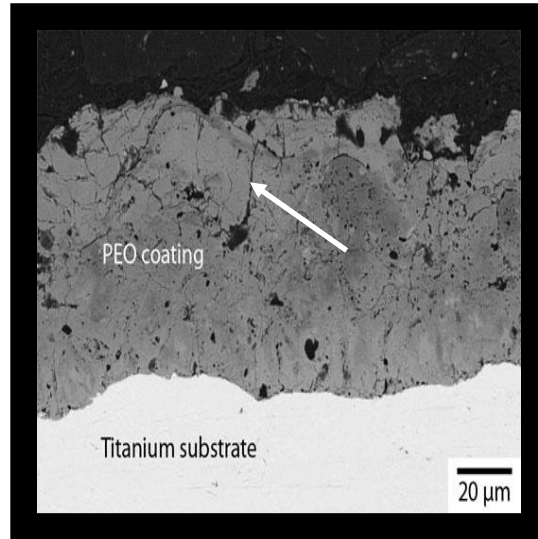
Figure 7: Micro Arc Oxidation (MAO) on a titanium substrate (grey formation) [44]. The white arrow points to the crack.

The anodizing method forms a pore less than 5 μm in size, extremely small compared to 150– 400 μm, the range of pore size usually used for experimental purposes. According to cell adhesion studies, the initial adhesion of the osteoblast is reported to be better in a micro-porous structure in comparison to a macroporous one [15,59]. Therefore, if a surface has a micro-porous structure, the filopodia extension of the osteoblast facilitates cell attachment.

The porous structure and the incorporation of calcium and phosphate to the substrates have advantages of maximizing the surface of artificial joints. The compositional components of a surface are thought to provide a good environment for bone stability. These findings confirm the excellent results obtained using calcium and phosphate in cell proliferation, morphology, differentiation, adhesion molecule gene expression in comparison to the currently used surface treatment methods [18].

18

Nie *et al.,*[52] used micro arc discharge oxidation to develop a thick and hard oxide ceramic layer on a BS Al-6082 aluminium alloy. The phase composition and microstructure of the MAO coatings were investigated by XRD, SEM and EDX analyses. A number of adhesion and tribological sliding and impact wear tests were also performed. It was found that Al–Si–O coatings with a hardness of up to 2400 HV and with excellent wear resistance and load support could be formed. The thickness of the coatings significantly influenced the mechanical properties. In terms of tribological performance, the thicker coatings performed best in sliding, scratch and impact tests while thin coatings were also surprisingly effective in both impact and low-load sliding. Li *et al.,* [45] developed a functionalized Ti substrate treated with MAO to confer antibacterial properties and good biocompatibility. The objective was to achieve an implant surface that had biocompatibility to fibroblasts while inhibiting bacterial adhesion. Through cytotoxicity tests and the determination of antibacterial efficacy, the results showed that the surface of Ti treated with MAO had no cytotoxicity and good antibacterial efficacy against the most common microbial pathogens encountered in transcutaneous implant infections. It was found that proper modification of the substrate had no influence on the cytocompatibility of the material and increased the antibacterial efficacy of the material. Hence, MAO coatings demonstrated to have good potential in transcutaneous implant applications. Kim *et al.,* [37] demonstrated the possibility of using a MAO-EPD treatment to improve the biocompatibility of Ti implants, in which bioactive HA particles are incorporated into the coating layer. It was proposed to directly incorporate well-crystallized hydroxyapatite (HA) particles into the titanium oxide layer on Ti without significantly altering the micro-porous coating morphology. The strategy combined the principles of the MAO process with an electrophoretic deposition (EPD) process, which is often used to coat the surface of Ti materials with a HA layer. A porous TiO_2 layer was formed via the MAO process, while at the same time, negatively charged HA particles migrated toward the Ti anode through the EPD process. These particles then become incorporated into the pores formed in the TiO_2 layer, resulting in the formation of a bioactive HA-incorporated TiO_2 coating layer on the Ti substrate. Ethanol was added to the electrolyte containing the fine HA particles in order to retard the evolution of the gas at the anode, which would otherwise obstruct the attachment of HA particles. The morphology, composition and phase of the coating layer were examined at different ethanol concentrations in the electrolyte and applied voltages during the MAO-EPD treatment. The biological properties of the coating

layers were evaluated using *in vitro* cell growth and osteoblastic differentiation assays. The results suggest that, when ethanol is added to the electrolyte solution, a considerable number of hydroxyapatite particles were incorporated into the coating layer. The amount of hydroxyapatite increased slightly with increasing amounts of ethanol from 10 to 25 %. However, a slight decrease in HA was observed when an ethanol concentration higher than 50 % was used. The incorporation of HA particles into the coating layer significantly improved the biocompatibility of the Ti implant compared with that of the Ti substrate in an electrolyte solution without HA particles. All the specimens showed excellent cell attachment and proliferation, indicating a biologically favorable environment. These preliminary *in vitro* tests demonstrated that the MAO-EPD treatment can improve the osseointegration of Ti implants by incorporating bioactive HA particles into the coating layer.

Wang *et al.,* [72] determined that osseointegration and bone formation along an implant surface consist of 3 stages: first, the recruitment and attachment of osteoblasts from the surrounding bone tissue; second, the proliferation and differentiation of osteoblasts; and finally, the synthesis and mineralization of a collagenous bone matrix. Wang and colleagues hypothesized that electro-deposited calcium phosphate (CaP) on chitosan coatings can enhance the proliferative ability and differentiation potential of osteoblasts. MC3T3-E1 cells were cultured on these CaP coatings. It was found that MC3T3-E1 cells cultured on the electrodeposited CaP/chitosan coatings had cell proliferation rates higher than those on the electrodeposited CaP coatings. At the same time, it was determined that alkaline phosphatase activity and collagen expression were increased, and both bone sialoprotein and osteocalcin genes were up-regulated. Additionally, no significant difference was found between the CaP/chitosan coatings. The results obtained suggested that the electrodeposited CaP/chitosan coatings enhance the proliferation and differentiation of MC3T3-E1 cells. These findings have great potential for future applications. Also, electrodeposited CaP/chitosan coatings have been demonstrated to improve bone marrow stromal cell attachment [56,72]; therefore, the coating can also enhance the proliferation and differentiation of osteoblast cells.

This method fundamentally combines the advantages of MAO with those of EPD. In particular, at the early stage of the treatment, a porous TiO_2 layer is produced using the MAO process. When the arc is reduced, HA particles are also incorporated into the titanium substrate. The incorporation of HA particles into the coating layer significantly improved the

biocompatibility of the Ti implant compared with that of the pure Ti substrate and the Ti substrate treated by MAO at 270 V in an electrolyte solution without HA particles. All the specimens showed excellent cell attachment and proliferation indicating a biologically favorable environment. On the other hand, the ALP activity was strongly affected by the microstructure and chemical composition of the coating layer. The ALP activity was increased by coating the surface of the Ti substrate with a porous TiO_2 layer using the MAO process due to the creation of a rough, biocompatible surface [32]. The ALP activity was increased further by incorporating bioactive HA particles into the porous TiO_2 coating layer through the MAO-EPD treatment. These preliminary *in vitro* tests demonstrated that the MAO-EPD treatment can improve the biocompatibility of Ti implants by incorporating bioactive HA particles into the coating layer. In addition, it should be noted that the HA-incorporated TiO_2 coating layer would be expected to provide excellent corrosion resistance. This paper demonstrated the possibility and effectiveness of a MAO-EPD treatment for the production of a bioactive HA-incorporated TiO_2 coating layer on the surface of Ti implants. The addition of ethanol to the electrolyte solution inhibited gaseous emission at the anode generated by the electrolysis of water, and allowed the efficient incorporation of HA particles into the porous TiO_2 coating layer during deposition. This in situ coating method is expected to provide strong bonding between the incorporated HA particles and TiO_2 phase formed by MAO of the Ti substrate. The *in vitro* tests showed a considerable increase in ALP activity after the MAO-EPD treatment compared with the specimens before and after the MAO treatment.

3. Objectives

3.1 General objective

- The main objective of this research was to determine the effect of nanotopography on the cytocompatibility of hFOB 1.19 osteoblasts grown on micro arc oxidized γ-TiAl and Ti-6Al-4V alloys.

3.2 Specific objectives

- Evaluation and comparison (qualitatively) of human fetal osteoblast morphology and adhesion on micro arc oxidized (MAO) γ-TiAl and Ti-6Al-4V (MAOTiV and MAOGTi) and on thermally oxidized Ti-6Al-4V and γ-TiAl at 500°C (TiV5 and GTi5) and 800°C (TiV8 and GTi8) disks using Scanning Electron Microscopy (using SEM).

- Evaluation and comparison (quantitatively) of human fetal osteoblast differentiation on micro arc oxidized (MAO) γ-TiAl and Ti-6Al-4V (MAOTiV and MAOGTi) and on thermally oxidized Ti-6Al-4V and γ-TiAl at 500°C (TiV5 and GTi5) and 800°C (TiV8 and GTi8) disks using the Alkaline Phosphatase Assay (ALP).

- Characterization of the morphology of the coatings by Atomic Force Microscopy (AFM) to determine surface topography.

4. Materials and Methods

4.1 Preparation of titanium disks

γ-TiAl and Ti-6Al-4V disks of 7mm in diameter and with an approximate thickness of 1 mm were manually cut from machined rods, using a low speed saw (Buehler™). Their surfaces were prepared manually in an Ecomet 3 (Buehler™) by wet grinding with 240, 320, 600 and 1200 grit silicon carbide paper to create a rough surface. These metal disks were ultrasonically cleaned in 0.8% Alconox (Fisher, Pittsburgh, Pennsylvania) and 70% ethanol for 10 minutes each, while rinsing with de-ionized water between each application. Ti-6Al-4V and γ-TiAl disks (GTi) polished and cleaned as described previously, and subsequently sterilized by ultraviolet light (one hour each side) were used as negative controls. Glass coverslips were used as positive controls [Figure 8].The metal disks were dried and then oxidized by the micro arc process at constant temperature and voltage for the time of treatment established (3 or 4 minutes) [Figure 9 (a) and (b)]. They were then transported to the cell culture laboratory and placed in 48-well culture plates (Corning, Corning, New York). After placing the titanium disks in the 48-well culture plates, cells were seeded as described in section 4.9.
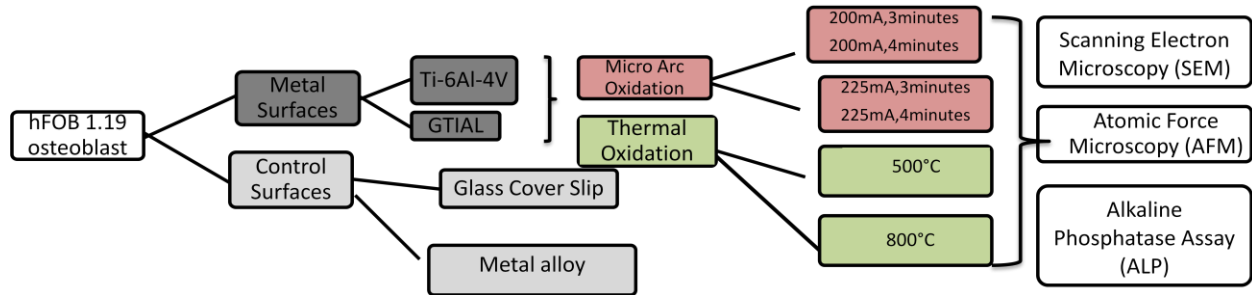
Figure 8: Setup used for the preparation of the titanium disks.

4.2 Thermal Oxidation Preparation

γ-TiAl [Ti–48Al–2Cr–2Nb (at.%)] and Ti-6Al-4V disks of 7 mm in diameter and thickness of 1 mm were manually cut from γ-TiAl rods and from machined wrought $(\alpha + \beta)$ Ti-6Al-4V annealed rods using a low speed saw (Buehler™). The surfaces were prepared manually in an Ecomet 3 (Buehler™) by wet grinding with 240, 320, 600 and 1200 grit silicon carbide paper to create a rough surface, and they were ultrasonically cleaned in 0.8% Alconox (Fisher) and 95% ethanol for 10 min each, while rinsing with deionized water between each cleaning process. The disks were dried and then oxidized in a laboratory furnace (CM Furnaces Inc.) in air at 500°C or at 800°C for 1 h. They were then transported aseptically to the cell culture laboratory and placed in 48-well cell culture plates (Corning). Thermally oxidized at 500°C and 800°C γ-TiAl and Ti–6Al–4V disks will be referred hereafter as GTi5, TiV5, GTi8 and TiV8, respectively.

4.3 Micro Arc Oxidation (MAO) Preparation

In the electrolytic cell used for all the processing conditions, the titanium sample acts as the anode, a stainless steel beaker is set as the cathode and used as a solution container as well. A *Hoeffer PS300-B* high voltage power supply (300V; 500mA) was used to produce the MAO coatings on both alloys [Figure 9 (a) and (b)].
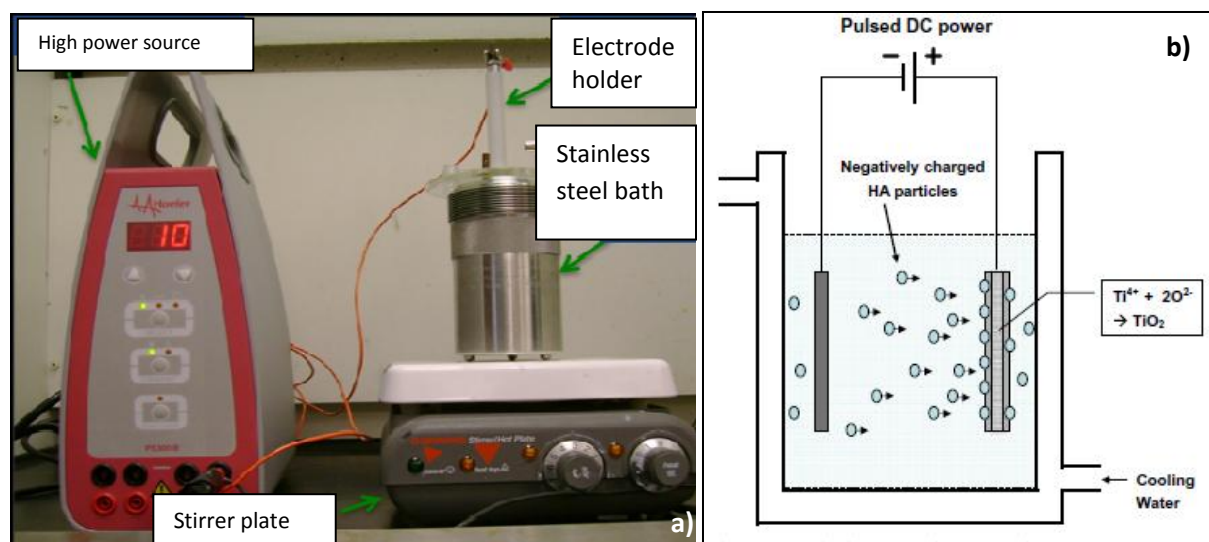
Figure 9: a) Instrumentation used for MAO treatment on Ti alloys [45]. b) Representation of electrolyte solution [42].

4.4 Electrolyte preparation

The electrolyte solution was prepared according to Frauchiger and colleagues [22], where calcium dihydrogen phosphate [$Ca(H_2PO_4)_2$] (0.025 molarity), calcium acetate [$Ca(OOCCH_3)_2$] (0.075 molarity), and $Na_2(EDTA)$ (0.12 molarity) was dissolved in ultra-pure water. The basic component of the electrolyte was calcium dihydrogen phosphate with a Ca/P ratio of 0.5. In order to increase this ratio in the solution, a chelating agent $Na_2(EDTA)$ was added to increase calcium ions to augment the Ca/P ratio in the coating. The electrolyte used consisted of an aqueous solution of phosphate (0.05 M) and calcium (0.1M), the latter in chelated form due to the formation of a complex. The EDTA concentration in the electrolyte was 0.12 M. In order to efficiently prepare the electrolyte, the pH of the solution was taken into consideration. Table 1 indicates the composition of the electrolyte. Each reactant (high purity grade) was dissolved in different containers until complete solubility was achieved, and then mixed according to the order indicated in Table 1. NaOH pellets were added for a pH of 11.

Table 1: Chemical composition of the calcium/phosphate electrolyte used in the MAO process.

Reactant	Quantity
Na$_2$-EDTA	44.67g/L
Calcium Acetate Ca(CH$_3$ COO)$_2$	12.76 g/L
Calcium Dihydrogen Phosphate Ca (H$_2$PO4)$_2$. H$_2$O	6.3 g/L

4.6 Experimental design

A preliminary test was performed [40] where different current density and time variables were considered [Table 2], and the final experimental design was made based on the analysis of the resulting coatings using the optical microscope. It was clearly established that current density and the time significantly affected the regularity and coating generated in both titanium alloys.

The different variables that were evaluated and subsequently used for experimentation are shown in Table 3.

Table 2: Preliminary parameters used for the treatment of MAO Ti-6Al-4V and γ-TiAl alloys.

	Ti-6Al-4V		γ-TiAl	
Condition	Current Density (mA/cm²)	Time (min)	Current Density (mA/cm²)	Time (min)
1	175	3	175	3
2	175	4	175	4
3	175	5	175	5
4	200	3	200	3
5	200	4	200	4
6	200	5	200	5
7	225	3	225	3
8	225	4	225	4
9	225	5	225	5

Table 3: Final experimental conditions used for MAO Ti-6Al-4V and γ-TiAl alloys.

	Ti-6Al-4V		γ-TiAl	
Condition	Current Density (mA/cm²)	Time (min)	Current Density (mA/cm²)	Time (min)
1	200	3	200	3
2	200	4	200	4
3	225	3	225	3
4	225	4	225	4

4.7 Micro arc oxidized (MAO) coatings

To fabricate the anodic oxidized samples, a stainless steel beaker was used as the cathode, and the titanium specimen was used as the anodic electrode. The sample was mounted in the titanium holder specially designed to allow complete exposure of the sample to the electrolyte [40]. The power supply was operated in galvanostatic mode in order to account for the increase in electrical resistance of the oxide film on the titanium surface with an increasing thickness. Voltage changes as a function of time were set manually for each condition used.

The MAO treated samples showed significant differences from bare samples. The coating was evident by visual inspection. After treatment, samples were rinsed with distilled water and then dried with a blow dryer for further characterization.

4.8 Morphological Characterization of Micro arc oxidized (MAO) coatings

Optical microscopy was used for preliminary visual characterization of the topography generated. An optical microscope *NIKON eclipse 80i* was used to obtain micrographs from γ-TiAl and Ti-6Al-4V alloys subjected to the MAO process. The conditions corresponding to the final experimental design were characterized further by using Scanning Electron Microscope JEOL-JSM-5410 LV SEM (JEOL, Japan).

4.9 Cell line

Human osteoblast cells, cell line hFOB 1.19 (ATCC, Manassas, Kansas), were cultured in 90% Dulbecco's Modified Eagle's Medium Nutrient Mixture F-12 Ham (DMEM) (Sigma-Aldrich, St. Louis, Missouri) with 2.5 mM L-Glutamine and 15 mM Hepes, without phenol red, supplemented with 0.3 mg/mL G-418 (Calbiochem, San Diego, California) and 10% Fetal Bovine Serum (FBS) (Hyclone, Logan, Utah). Cells were grown in 25 cm² plastic culture flasks (Corning, Corning, New York) and incubated at 33.5°C until confluence. At approximately 100% confluence, cells were washed three times with Phosphate Buffer Saline solution (PBS) (137mM NaCl, 2.7 mM KCl, 4.3 mM Na_2HPO_4, 1.4 mM KH_2PO_4) and harvested using 0.25% trypsin- 0.53mM EDTA (Gibco, Gaithersburg, Maryland) at 37°C for 5 min. Cells were then pelleted by low speed centrifugation (3,300 rpm) for 5 minutes and subcultured at a 1:3 ratio

[6].Cells were seeded in 48-well plates at a density of 5 x 10^4 cells/cm². Samples were then incubated for 3 days, followed by 7 days at 39.5°C.

5.0 Scanning Electron Microscopy Analysis (SEM)

Cell adhesion on all of the Ti-6Al-4V and γ-TiAl alloys were evaluated qualitatively by SEM. Thermally oxidized Ti-6Al-4V and γ-TiAl alloys at 500°C and 800°C (TiV5,TiV8, GTi5,GTi8) were used for comparison. Cells were seeded in 48-well plates (Becton- Dickinson, Lincoln Park, NJ) at a density of 5 x 10^4 cells/cm² on TiV, TiV5, TiV8, GTi, GTi5,GTi8, MAOTiV and MAOGTi disks (7mm in diameter). Samples were incubated for 3 days at 33.5°C and then for 7 days at 39.5°C. TiV, TiV5, TiV8, GTi, GTi5, GTi8, MAOTiV and MAOGTi disks were incubated with and without culture media (negative control). Cells were also grown on coverslips. After the incubation period, samples were washed carefully with PBS and fixed overnight in 4% glutaraldheyde buffered in PBS at 4°C. After washing three times in PBS, the samples were dehydrated in graded alcohol ranging from 10% to 100% ethanol in intervals of 10 minutes each. After critical point drying (EMS 850) (Electron Microscopic Science, Washington), samples were mounted on stubs and sputter-coated with gold palladium in EMS 550X (Electron Microscopic Science, Washington). Samples were then examined with a JEOL JSM-5410 LV SEM (JEOL, Japan) at 10 KV using different magnifications (150, 1000, 3500 and 5000X).

5.1 Alkaline Phosphatase Assay (ALP)

To evaluate osteoblast differentiation quantitatively on thermally oxidized and micro arc oxidized γ-TiAl and Ti-6Al-4V disks, cells were seeded in 48 well plates (Becton, Dickinson, Lincoln Park, NJ) at a density of 5 x 10^4 cells/cm² on TiV, TiV5, TiV8, GTi, GTi5,GTi8, MAOTiV and MAOGTi disks (7mm in diameter); using the Alkaline Phosphatase Colorimetric Assay Kit (ab83369, Abcam®). Samples were incubated for 3 days at 33.5°C and then for 7 days at 39.5°C. Cells were also grown on coverslips. Modifications to the protocol included washing the samples carefully three times with PBS and homogenizing in 60 μL of the Assay Buffer. Another modification made was the use Triton X-100 (80 μL) to lyse the cells for an efficient measurement of intracellular ALP. The solution in each well (from the 48 well plate mentioned

above) was transferred to a 96-well plate (Becton-Dickinson, Lincoln Park, NJ). A Solution (50 µl) of pNPP was added to each well containing the test samples and background controls. The reaction was incubated for 60 minutes at 25 °C and protected from light. The stop solution (20 µL) was added to terminate ALP activity in the sample. The Optical Density was measured at 405 nm in a micro plate reader [Figure 10].
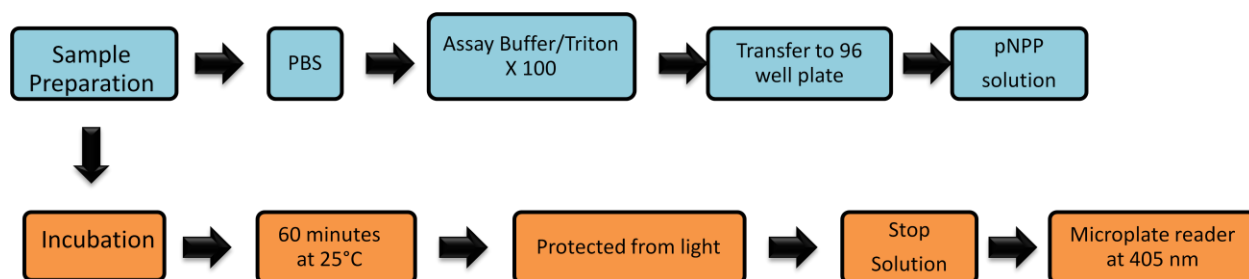
Figure 10: Methodology used for ALP assay on Ti-6Al-4V and γ-TiAl alloys.

A standard curve was generated to determine the concentration of ALP activity in the sample: 40 µl of the 5 mM *p*NPP solution was diluted in 160 µl Assay Buffer to generate a 1 mM *p*NPP standard. 0, 4, 8, 12, 16, 20 µl were added into a 96-well plate in duplicate to generate 0, 4, 8, 12, 16, 20 nmol/well *p*NPP standards. The final volume was brought to 120 µl with Assay Buffer. ALP enzyme solution (10 µl) was added to each well containing the *p*NPP standard. The reaction was incubated for 60 minutes at 25°C and protected from light [Figure 11]. All reactions were stopped by adding 20 µl Stop Solution into each standard and sample reaction except the sample background control reaction (since 20 µl Stop Solution had been added to the background control when prepared previously). The Optical Density was measured at 405 nm in a micro plate reader. The background was corrected by subtracting the value derived from the 0 standard from all standards, samples and sample background control. The *p*NPP Standard Curve was plotted and the sample readings were applied to the standard curve to get the amount of *p*NPP generated. ALP activity of the test samples was calculated using the following equation:

ALP activity (U/ml) = A/V/T

Where A is amount of *p*NPP generated by samples (in μmol).

V is volume of sample added in the assay well (in ml).

T is reaction time (in minutes)
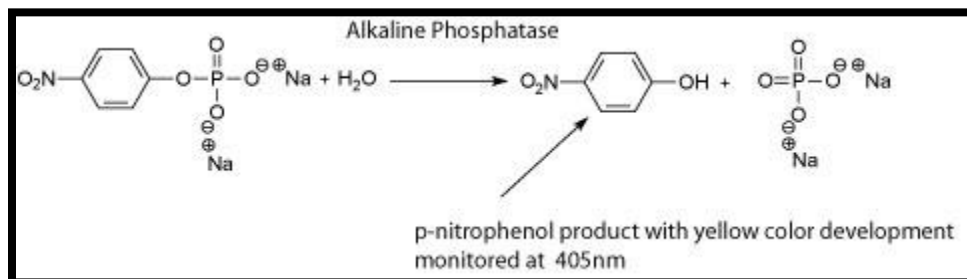
Figure 11: Alkaline Phosphatase Chemical Reaction [21].

5.2 Statistical Analysis

The alkaline phosphatase assay was performed in three independent experiments, each with three replicates, for a total of nine replicates per surface evaluated (micro arc oxidized GTi, thermally oxidized GTi, GTi, micro arc oxidized Ti-6Al-4V, thermally oxidized Ti-6Al-4V, Ti-6Al-4V and glass coverslips) for a 10 day culture period. The data of the alkaline phosphatase assay is presented as the mean ± standard deviation (S.D.) of the optical density of the differentiated cells on the different surfaces and the amount of alkaline phosphatase detected. Each value represents the mean (using three disks) of cell differentiation performed on a specific surface tested in one of the three independent experiments. A factorial analysis of variance (ANOVA) was used to assess the main effect and the significant interactions between the type of metal (γ-TiAl or Ti-6Al-4V), and type of surface treatment (micro arc oxidization at 200mA, 3min., 200mA, 4min., 225mA, 3min. and 225mA, 4min., thermal oxidization at 500°C and 800°C. When these interactions were found, they were graphically analyzed. In addition, a Randomized Complete Block Design (RCBD) was performed to reduce the variance in the data. A "Block" is a set of homogeneous experimental units (similar to each other). This design was

used to randomly assign treatments to the samples within each block so that each treatment was represented three times (triplicate) in each block. This guarantees that all treatments are represented in all blocks, and that comparisons are free of the differences between blocks. Then, the experimental design was implemented within each block or homogeneous subgroup. A contrast test was performed to compare the type of metal (γ-TiAl and Ti-6Al-4V) with the surface treatments. Additionally, to check for the presence of significant differences in cell differentiation on the type of metal and surfaces tested, a LSD Fisher test was performed. A Fisher's least significant difference (LSD) test is a two-step testing procedure for means comparisons of several treatment groups. In the first step of the procedure, a global test is performed for the null hypothesis that the expected means of all treatment groups under study are equal. If this null hypothesis can be rejected at a specified ($p < 0.05$) level of significance, then means comparisons of all treatment groups are made at the same level of significance. The *p* values < 0.05 were considered to be statistically significant. All analyses were performed using Infostat® (Infostat Inc).

5.3 Atomic Force Microscopy (AFM)

Atomic Force Microscopy was used to characterize the surface topography of the coatings obtained on both titanium alloys. *Nansosurf Easy Scan 2 flex AFM* was used for this purpose under static force mode, with a spring constant value of 0.2 N/m. Contact mode was used for topography imaging.

In order to relate the results obtained by AFM, roughness measurements were carried out by using SJ-201 surface roughness tester. The results reported correspond to the average value of 8 measurements taken at different sites on each specimen [40].

6.0 Results and Discussion

Numerous variables influence the biocompatibility and osteogenic potency of nanostructured biomaterials *in vitro* and *in vivo*. The surface topography and the composition of a biomaterial affect cellular attachment, adherence, proliferation and migration, and also differentiation and survival of defined cell types. Chemical composition, surface structure (topography, geometry, roughness, and particle size), surface energy, hydrophobicity, and the degree of solubility in aqueous solutions of a biomaterial will define an implant regarding its osteoblast promoting potency. Therefore, a complete characterization of the topography or coating features has to be performed in order to understand the process of the coating formation and relate this information to the current density and time of exposition to treatment and how this affects cell behavior. Both alloys (γ-TiAl and Ti-6Al-4V) were subjected to MAO treatments following the experimental conditions described in Table 3. A thorough comparison is made between the results obtained for each characterization technique.

6.1 Preliminary experimentation for micro arc oxidation (MAO) conditions

The variables considered in this study were current density and time of exposure to treatment. Selection of the final experimental design was made based on the analysis of the coatings with optical microscopy. Optical microscopy was used to identify changes in coating characteristics with the increase of current density in order to establish the parameters to be used in the experimental design. It was established that current density and time of exposition to treatment affects the coating features in Ti-6Al-4V and γ-TiAl alloys [40]. Li *et.al.,* [42] determined that these features are due to the complex formation from Ca^{2+} to $[Ca.Y]_2$ and has two main consequences:

1. The solubility of Ca is increased, preventing the precipitation of calcium phosphate at high calcium concentrations.
2. The positively charged calcium ions are converted to negatively charged $[Ca.Y]^{2-}$ ions, which are attracted (instead of being repelled like Ca^{2+}) by the positively polarized titanium electrode during the micro arc oxidation process.

It was also noticed that the order in which the solutions were combined in preparation of the electrolyte solution had a significant effect in the interactions between dissociated ions affecting the complex formation of positively charged calcium ions to negatively charged ions which is crucial in further processing [42].

Differences in the resulting porosity and topography of the oxide layers were observed for each alloy as the current density values changed. A similar response to the increase in current density was noticeable, yet different values to reach dielectric breakdown of the growing film was observed for the alloys. Values used in the MAO process for Ti-6Al-4V were slightly higher than those for γ-TiAl. This phenomenon can be related to the different compositions and microstructures of the alloys, Ti-6Al-4V alloys exhibit a duplex (α+β) structure and γ-TiAl alloys consist mainly of 80% lamella and 20% blocky γ grains [40,51]. The specific characteristics of the oxide films growing on each alloy (different electric resistivity and other electric properties as thickness changes) can account for these differences, in agreement with the results obtained by Song *et al.,* [65] in different titanium alloys.

For γ-TiAl samples, dielectric breakdown is not observed until the current density of 150mA is reached whereas for Ti-6Al-4V it is reached at 175mA. Beyond a current density of 300mA, material destruction and dissolution of the coating can be observed.

When current is applied without reaching the dielectric breakdown, the alloys are subjected to normal anodic oxidation. Depending on the thickness of the oxide film formed on each alloy in response to these parameters used (specific for each alloy as seen in Figures 12 and 13, a-h) different coloration is observed. Coating on the surface of the metal substrates was evident based on the different colors exhibited in the anodic oxide films. For γ-TiAl, this behavior was observed at a lower current density. After dielectric breakdown, the coating is highly porous and differs significantly from the features observed for anodic oxidation. Further increase of the current density leads to material destruction and selective dissolution of the preexisting coating [40]. Based on these observations, a range of variables [200mA, 3min, 200mA, 4min, 225mA, 3min, and 225mA, 4min] were selected to obtain conditions for micro arc oxidation; with the goal of obtaining coatings which are uniformly distributed over the sample surface while avoiding values that may cause oxide film dissolution and therefore a non-uniform coating.

Ti-6Al-4V γ-TiAl
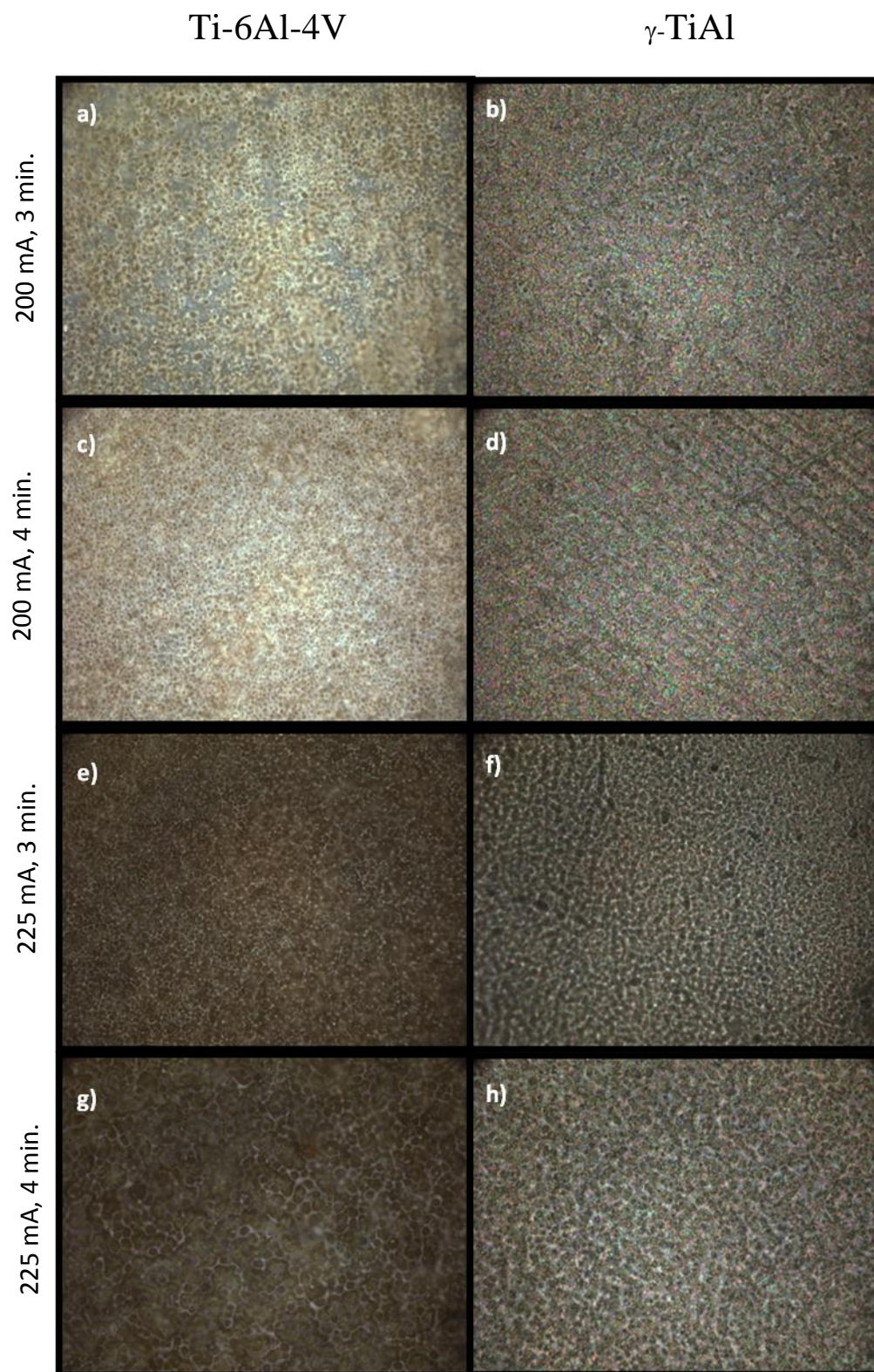
Figure 12: Optical microscopy of MAO Ti-6Al-4V and γ-TiAl alloys at 50 x. The conditions that were evaluated were: a, b) 200mA, 3min c, d)200mA, 4min e, f)225mA, 3min and g, h) 225mA, 4min.

Ti-6Al-4V   γ-TiAl
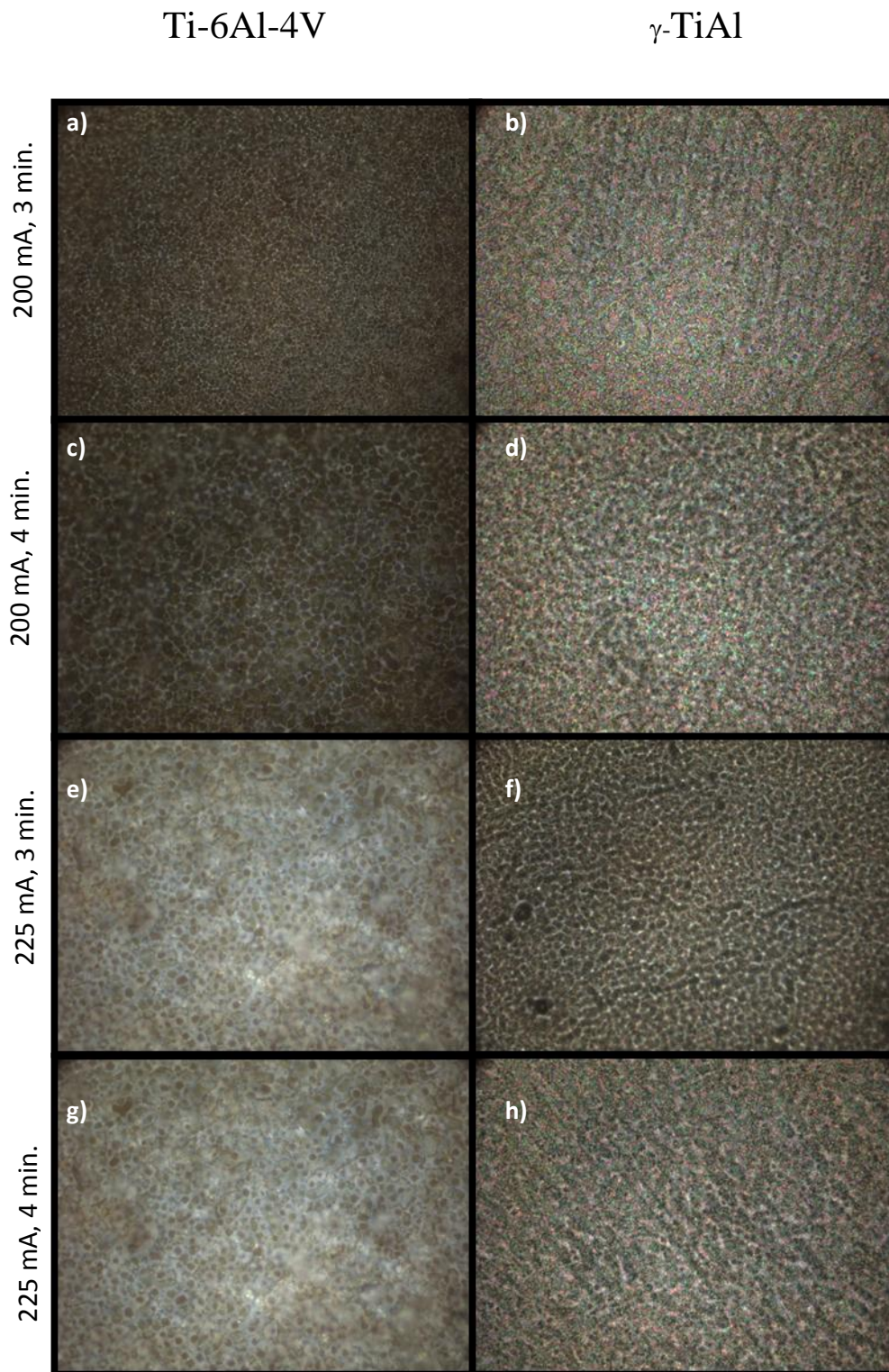
Figure 13: Optical microscopy of MAO Ti-6Al-4V and γ-TiAl alloys at 100 x: The conditions that were evaluated were: a, b)200mA, 3min c, d)200mA, 4min e, f)225mA, 3min and g, h)225mA, 4min.

6.2 Scanning Electron Microscope (SEM Analysis)

Micro arc oxidized titanium alloys were evaluated to determine its possible applications as an implant material. hFOB 1.19 cell growth on micro arc oxidized γ-TiAl and Ti-6Al-4V was also observed for different surface roughness. SEM examination was used to qualitatively access cell attachment on the different surfaces. Excellent cellular activity on material surfaces, suggested by SEM imaging, can be attributed to the presence of cellular deposits and growth, attachment, and proliferation of cells during *in vitro* conditions.

Images obtained by SEM [Figures 16 through 19] are shown with and without cell culture incubated for 3 days at 33.5° C and 7 days at 39.5° C on glass coverslips, micro arc Ti-6Al-4V and γTiAl surfaces and thermally oxidized Ti-6Al-4V and γTiAl surfaces. These images were captured at 150X, 1000X, 3500X and 5000X magnifications.

Figures 14 and 15 [a through f] show the SEM images obtained for all Ti-6Al-4V and γ-TiAl samples without cell culture. The SEM images of GTi and TiV exhibit a smoother surface compared to the other samples [Figure 15 (a) and (b)]. In addition, this passive oxide layer covered the parallel grooves and striations that are still visible on GTi [black arrow, Figure 15 (b)]. This was generated by the wet grinding procedure previously described in section 4.1 and 4.2. Rounded surface structures of the metal were visible in TiV5, suggesting clusters of oxide granules present [white arrow, Figure 15 (c)].

The SEM images of GTi8 and TiV8 without cells exhibited a rougher surface compared to the other samples [Figure 15 (e) and (f)]. Bigger oxide granules were present on TiV8 [Figure 15 (e)] compared to those of GTi8 [Figure 15 (f)], conferring an irregular appearance to this surface suggesting that TiV8 oxide layer is thicker than the other oxide layers evaluated.
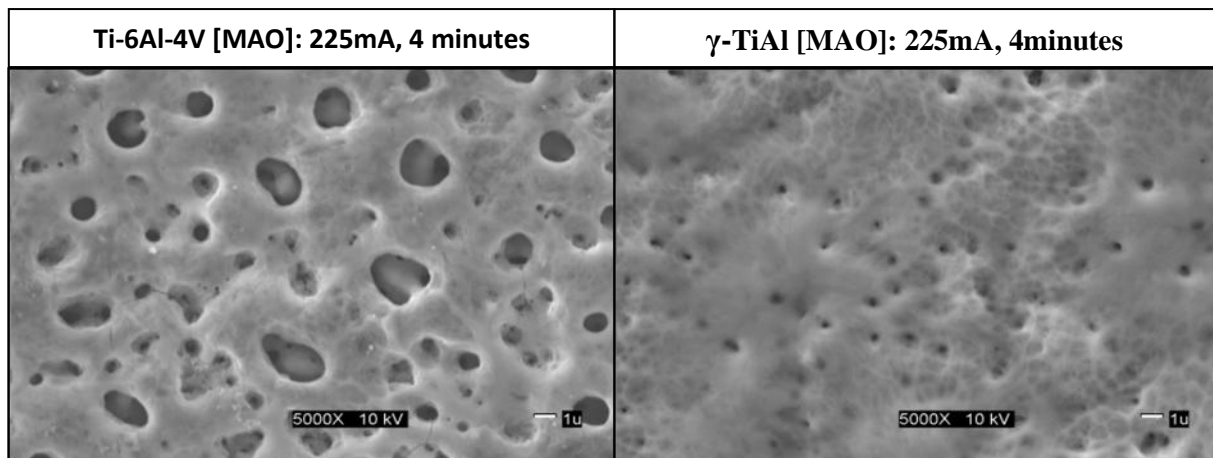
Figure 14: SEM images of the Micro Arc Oxidized Ti-6Al-4V and γ-TiAl alloys.
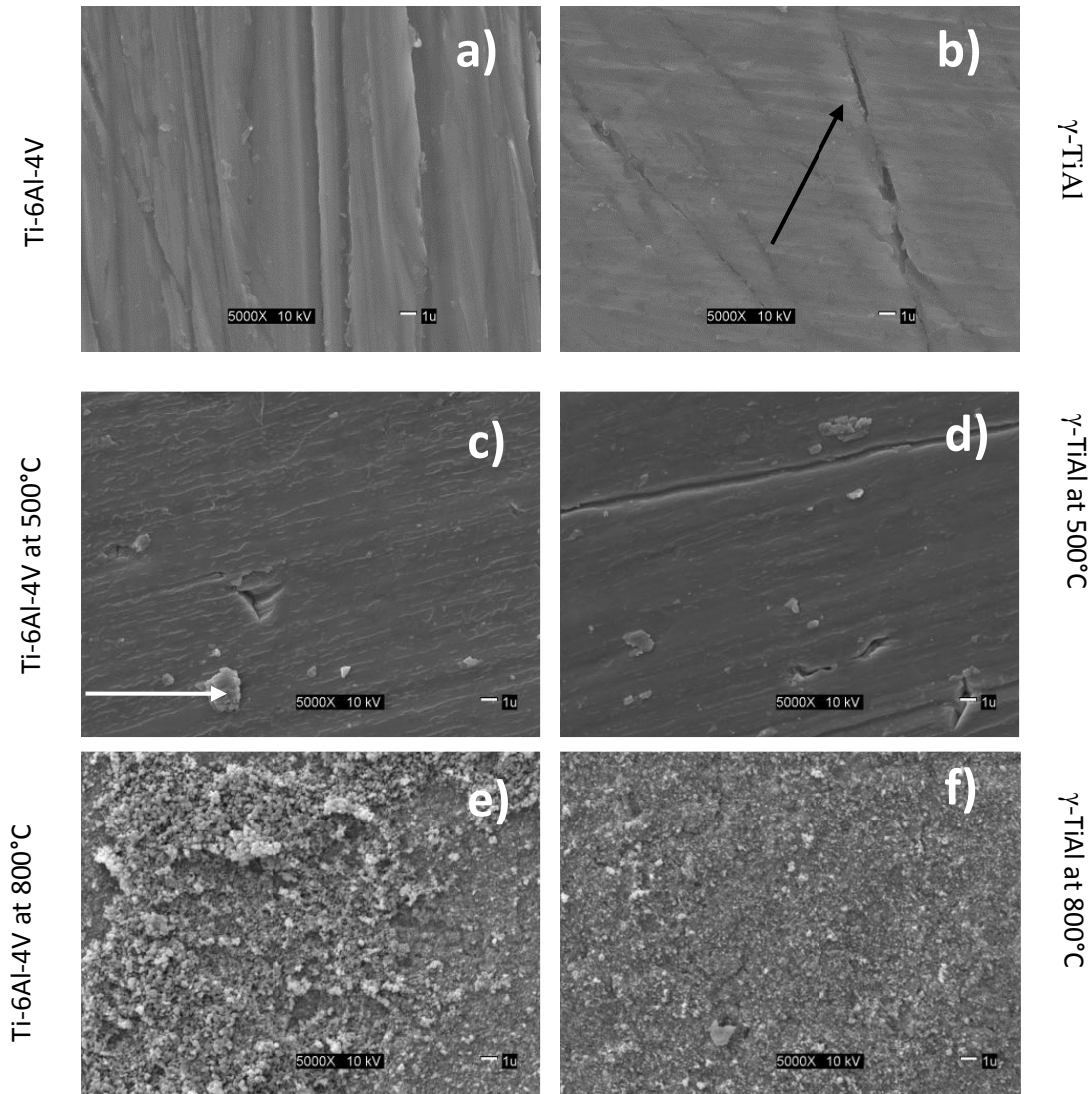
Figure 15: SEM micrographs of Ti-6Al-4V and γ-TiAl alloys. (a), (b), (c), (d), (e) and (f): (a) and (b) represent Ti-6Al-4V and γ-TiAl alloys without treatment. (c), (d), (e) and (f) represent Ti-6Al-4V and γ-TiAl alloys treated with thermal oxidation. The white arrow points to the rounded surface structures on the metal. The black arrow show a parallel groove generated on the metal.

Scanning Electron Microscopy analysis showed that hFOB 1.19 cells grew on the surface of both γ-TiAl and Ti-6Al-4V disks. Differences in cell attachment and behavior were observed for hFOB 1.19 cells cultured on micro arc oxidized γ-TiAl and Ti-6Al-4V alloys. Cell attachment and proliferation was similar between both metals. The cell growth control sample [Figures 16 through 19] allowed us to observe cell confluence, growth, and attachment under *in vitro* conditions.

The osteoblast cells were spread and flattened on the glass surfaces. The osteoblast cells exhibited such close contact with each other that detection of cellular boundaries was difficult [Figure 16]. Fibrous networks, which may correspond to fibrillar collagen, the main component of bone extracelluar matrix (ECM), allows the adhesions of cells and is important for the proper assembly of the extracellular matrix. The extracellular matrix has several functions, such as a calcium phosphate reservoir, support, protection, and in homeostasis [6]. In addition, nodules of mineralization with a sponge-like morphology were scattered through the samples. Many nodules of mineralization intimately associated with the fibrillar network were observed [white oval, Fig. 19]. The maturation of the extracellular matrix (ECM) is evidenced by the presence of fibrous networks associated with cells and an increase in nodules of mineralization. Also, small mineral deposits on the glass surface can clearly be noticed. These deposits can be attributed to inorganic constituents (inorganic salts), specifically to crystalline solids compounds containing DMEM and FBS used for the growth of osteoblasts *in vivo*. It is believed that these nodules of mineralization can be composed of elements such as C, O, P, Ca and Ti waste as reported by Advincula *et al.,* [1]. Also, these nodules of mineralization can be composed of the components of the electrolyte used for the preparation of the micro arc oxidized substrates which is mainly composed of calcium phosphate.

A direct comparison of the cells cultured on γ-TiAl and on Ti-6Al-4V alloys was performed [Figures 16 through 19]. Micro arc oxidized alloys were compared to thermally oxidized alloys to determine changes in the morphological characteristics of the coating that can potentially affect cell adhesion and biocompatibility. Slender cytoplasmic projections (filopodia) extended from the cells in all directions on micro arc oxidized Ti-6Al-4V and γTiAl disks treated with the four current densities and treatment time (200mA, 3min., 200mA, 4 min., 225mA, 3min., 225mA, 4 min.) [Figure 16]. This suggests adequate cell growth and allows evaluating the biocompatibility of implant materials [45]. In addition, sheet-like cytoplasmic protrusions

extending from the cell body in all directions were observed. This suggests the ability of cellular movement or spreading along the substrate and also demonstrates that cellular division (mitosis) may be occurring. Small rounded structures, likely mineralization nodules, were observed in Figure 16. The presence of mineralization nodules suggests the maturation of the ECM and the formation of bone-like tissue. There is an evident variation in the appearance of osteoblasts when cultured on the roughest and largest pores (Ti-6Al-4V) in comparison to the smoothest and small pores (γ-TiAl). This is a favorable feature since rough surfaces and highly porous coatings may enable bone osseointegration, producing lasting mechanical interlocking between the implant and bone, thus increasing service life of the implant.

Cells cultured on the smoothest surfaces of both γ-TiAl and Ti-6Al-4V [Figures 16 through 19] have a similar, if not identical appearance to that of cells grown on glass coverslips forming a continuous and confluent cell layer. Thickness of the cell layer due to the growth of a multi-cell layer was observed. Cells cultured on the roughest surface also achieved confluence, but the appearance of the cell layer was different from that of the control. Deligianni *et al.,* [18] determined that cell attachment and proliferation were sensitive to surface roughness and increased as the roughness of the Ti alloy increased. Cell attachment was observed on thermally and micro arc oxidized alloys; however increase in roughness of any substrate is dependent on the chemistry of the oxide as seen with the thermally oxidized alloys at 800°C. Therefore, roughness as well as the substrate plays an important role in determining the degree to which these cells attach and proliferate.

At higher magnifications, on the thermally oxidized Ti-6Al-4V and γTiAl alloys at 500°C, cell morphology and cellular interaction with the underlying surface was observed. This cellular interaction was observed by cellular attachment and proliferation. The multilayer was constituted by elongated and polygonal cells with some round shaped cells [Figure 19]. The presence of a few small rounded structures which may correspond to mineral nodules [red arrow, Figure 19] was noticed. At high magnification, the mineral nodule was in close contact with cells and had a sponge-like appearance. The presence of these mineral nodules can be attributed to the activity of osteoblasts in one of its functional stages of extracellular matrix after maturation. Furthermore, it is confirmed by Muller *et.al.,* [51] that at longer periods of incubation an abundant presence of these deposits is observed. However, Ti-6Al-4V and γ-TiAl thermally oxidized disks at 500°C also showed irregular and rounded surface structures [white rounded

square, Figure 19]. The black arrow in Figure 19 (500°C) points to a parallel groove or polishing mark caused in the process of preparation. Also, the surface oxide layer present on Ti-6Al-4V and γ-TiAl disks thermally oxidized at 500°C are characterized by the presence of a uniform coating with small irregular to rounded surface structures.

On the thermally oxidized Ti-6Al-4V alloys at 800°C, only irregular structures were observed. There was cell debris indicative of cytotoxicity of the oxide [white bracket, Figure 19]. This is possibly because of the release of harmful ions such as vanadium or by the formation of toxic compounds formed in the oxide layer by thermal oxidation. Membrane pores on the cell represents the process of cellular apoptosis. The mechanism consists in the release of a protease to the cytoplasm that is normally sequestered in the intermembrane space of mitochondria. Its release from the mitochondria occurs as a result of disruption of the outer mitochondrial membrane due to its swelling caused by an opening of transition pores in their inner membranes. This disrupts the outer mitochondrial membrane and releases the apoptosis-inducing protein. Consequently, these anchorage dependent cells become round and are not able to attach to the substrate. However, on thermally oxidized γ-TiAl alloys, fibrous networks and mineralized nodules were observed on elongated cells [white rectangle, Figure 19]. Most cells had elongated and polygonal morphologies. One plausible explanation for the lower cell attachment observed on TiV8 could be its irregular and potentially toxic surface [6], which did not promote a tight cell adhesion at day 3, thus favoring cell detachment in a time dependent manner and the consequent lack of cells on TiV8 at 10 days post seeding.

For micro arc oxidized γ-TiAl and Ti-6Al-4V alloys, cells are in direct contact with the substrate surface and, at higher magnifications, the cells appeared to have cellular extensions for anchorage. The presence of a fibrillar network and filopodia extensions are evident when cells were observed under higher magnifications on micro arc oxidized Ti-6Al-4V and γ-TiAl disks at a current density of 200mA with a treatment time of 3 minutes [white arrow, Figure 19]. Also, single cells had a flat appearance and a prominent nucleus area which is the typical appearance of osteoblast cells reported in the literature and references of osteoblast cells observed under SEM [27]. In a γ-TiAl sample, a mitosis-like structure could be observed [white inverted round bracket, Figure 18], with cells in the process of separating. This is also a clear indication that cells can grow and proliferate on micro arc oxidized γ-TiAl and Ti-6Al-4V alloys. An oval cell was observed on micro arc oxidized Ti-6Al-4V and γ-TiAl disks at a current density of 200mA

41

with a treatment time of 4 minutes [Figure 17]. This cell showed a ruffled surface and many filopodia in different directions.

A confluent multilayer of cells was observed at a current density 225mA with 3 minutes of treatment [Figure 16]. The multilayer was constituted by elongated and polygonal cells. The polygonal elongated cell morphology corresponds to the start of the cell-surface interaction processes such as anchorage and adhesion of the cell [29]. Also, cellular boundaries were difficult to establish due to the close contact between neighboring cells [white rounded rectangle, Fig. 16]. Some cells showed variable appearance (spherical, oval or polygonal) and some of the spherical cells grew over the elongated cells [6]. This cell had a rough surface but lacked cell projections. Also, cell-cell interactions were observed with the presence of cytoplasmic projections (mitotic like structures) and lamellipodia extending from the cells [inverted round bracket, Figure 18]. This lamellipodia is typical of migratory cells and are also part of the cytoskeletal organization which involves transport phenomena, cell division and helps extend the cell surface and improve the exchange of substances [29]. For this reason, the presence of cytoskeletal components on the cells indicates normal cell activity.

The ECM was more fibrillar on the micro arc oxidized Ti-6Al-4V and γ-TiAl disks with the highest current density (225mA with 4 minutes of treatment) [Fig.16 through 19]. The rounded cell shown in Figure 19, exhibited a ruffled surface and many filopodia in multiple directions. This cell was in close contact with the underlying cell layer and substratum through filopodia [Figure 19]. Moreover, some polygonal and spherical cells were also observed in Figure 19.

After 10 days of incubation, a confluent multilayer of cells was observed [Figures 16 through 19]. When cells were seeded on disks, SEM images showed that after this incubation period (3 days at 33.5ºC and subsequently 7 days at 39.5ºC) hFOB 1.19 cells were attached on glass coverslips as well as on MAOGTi, GTi5, Gti8, MAOTiV and TiV5 disks, but they did not adhere to TiV8 disks. The osteoblast cells formed confluent cultures on all the surfaces, except on TiV8. The oxide layer present on γ-TiAl and Ti-6Al-4V thermally oxidized disks at 800°C were very granular, resulting in a rough surface. However, the oxide granules formed on Ti-6Al-4V disks at 800°C were bigger in comparison to the granules formed on γ-TiAl disks at 800°C, resulting in a rougher appearance of the sample.

At lower magnifications, cells appeared to spread and anchor on both metal surfaces, independently of their roughness. On smoother surfaces or less porous surfaces (micro arc oxidized γ-TiAl), cells had a more flattened appearance, this likely a direct result of the smooth surface of the metal, whereas on the more porous surfaces (micro arc oxidized Ti-6Al-4V) topography is similar to that of the underlying metal.

Based on these results, the presence of the oxide layer on Ti surface can play an important role in biocompatibility and chemical properties. The use of micro arc oxidation has its benefits, such as the oxide coating being thicker and more bioactive than that resulting from thermal oxidation.

The type of electrolyte used and electric conditions applied can be altered to affect the surface morphology, chemical composition, and crystalline structure of the oxide coatings formed by MAO. Although there are many reports of outstanding clinical results on the bioactivity of micro arc oxidized titanium alloys and its use as artificial joints in the human body; and it is expected to be widely applied to implants of human body MAO does not contain the adequate composition components, hydroxyapatite like the human bones [18]. Moreover, very little data exists on the nature of direct cellular interaction with MAO treatment surfaces. Therefore, more information is needed about the early factors involved in the osseointegration process and the importance of osteoblast spreading and adhesion to MAO, especially in comparison to different surfaces.

Coverslip	Metal alloy	Thermal Oxidation		Micro Arc Oxidation			
Positive control	Negative control	500° C	800° C	200 mA, 3 min.	200 mA, 4 min.	225mA, 3 min.	225mA, 4 min.
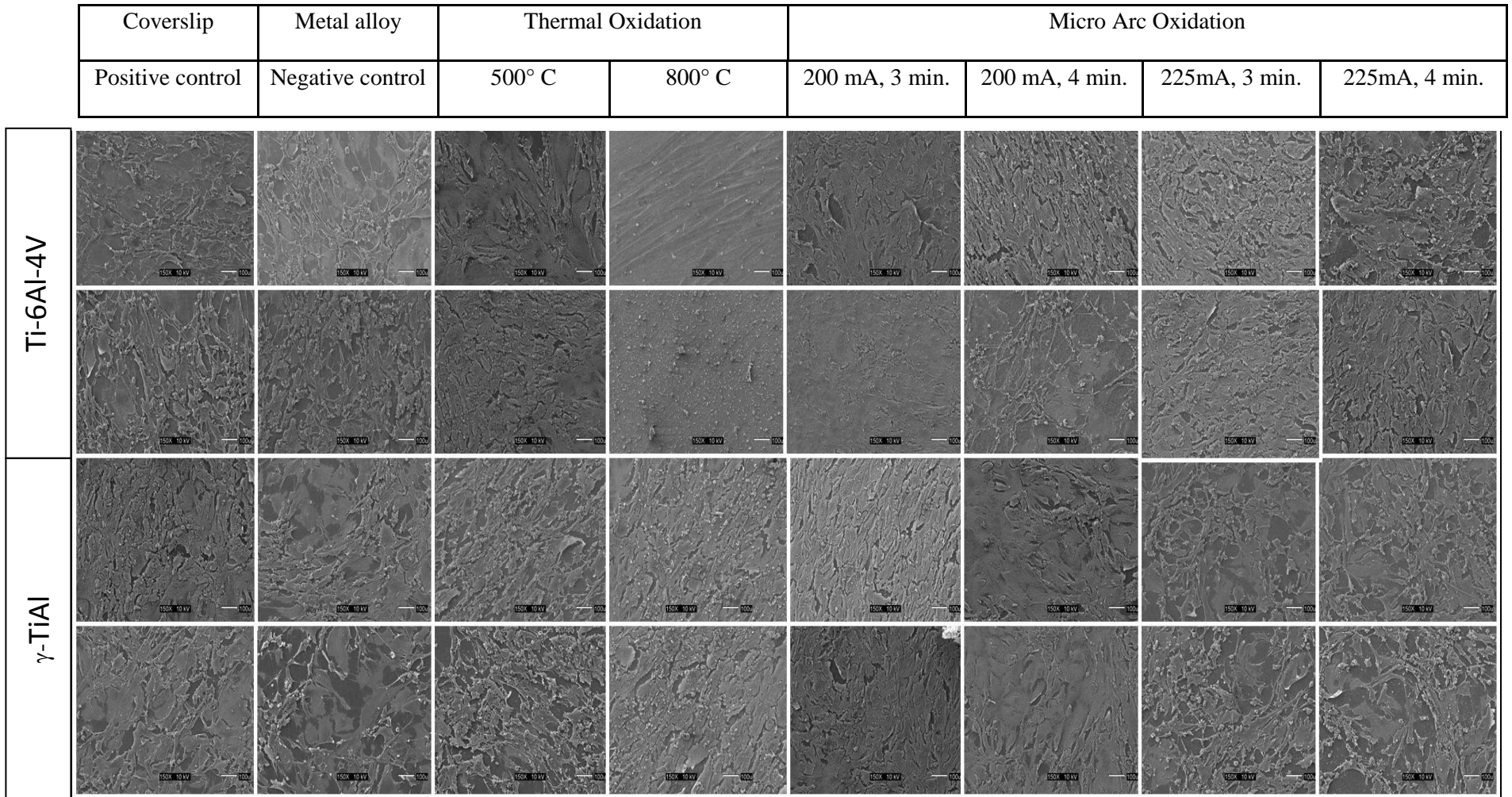
Figure 16: SEM micrographs of hFOB 1.19 cells on a glass coverslip (positive control), GTi and TiV (negative controls), TiV5 and GTi5 (500°C), TiV8 and GTi8 (800°C), MAOTiV (200mA and 225mA at 3 min and 4 min), MAOGTi (200mA and 225mA at 3 min and 4 min) disks. Each column shows the cell appearance by SEM on each surface at the magnification of 150X. (Scale bar: left and center 10μm, right 1μm).

44

Coverslip	Metal alloy	Thermal Oxidation		Micro Arc Oxidation			
Positive control	Negative control	500° C	800° C	200 mA, 3 min.	200 mA, 4 min.	225mA, 3 min.	225mA, 4 min.
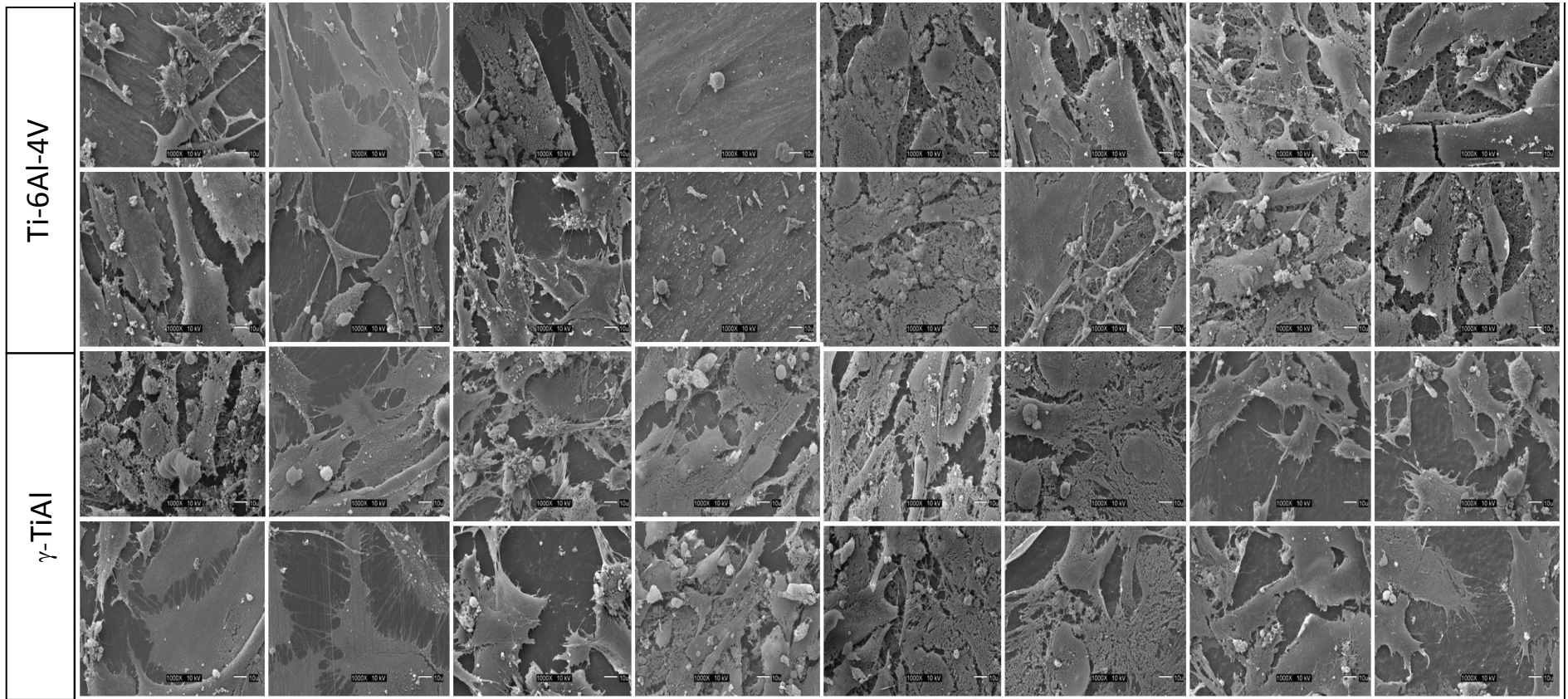
Figure 17: SEM micrographs of hFOB 1.19 cells on a glass coverslip (positive control), GTi and TiV (negative controls) , TiV5 and GTi5 (500°C), TiV8 and GTi8 (800°C), MAOTiV (200mA and 225mA at 3 min and 4 min), MAOGTi (200mA and 225mA at 3 min and 4 min) disks. Each column shows the cell appearance by SEM on each surface at the magnification of 1000X. (Scale bar: left and center 10μm, right 1μm).

45

Coverslip	Metal alloy	Thermal Oxidation		Micro Arc Oxidation			
Positive control	Negative control	500° C	800° C	200 mA, 3 min.	200 mA, 4 min.	225mA, 3 min.	225mA, 4 min.
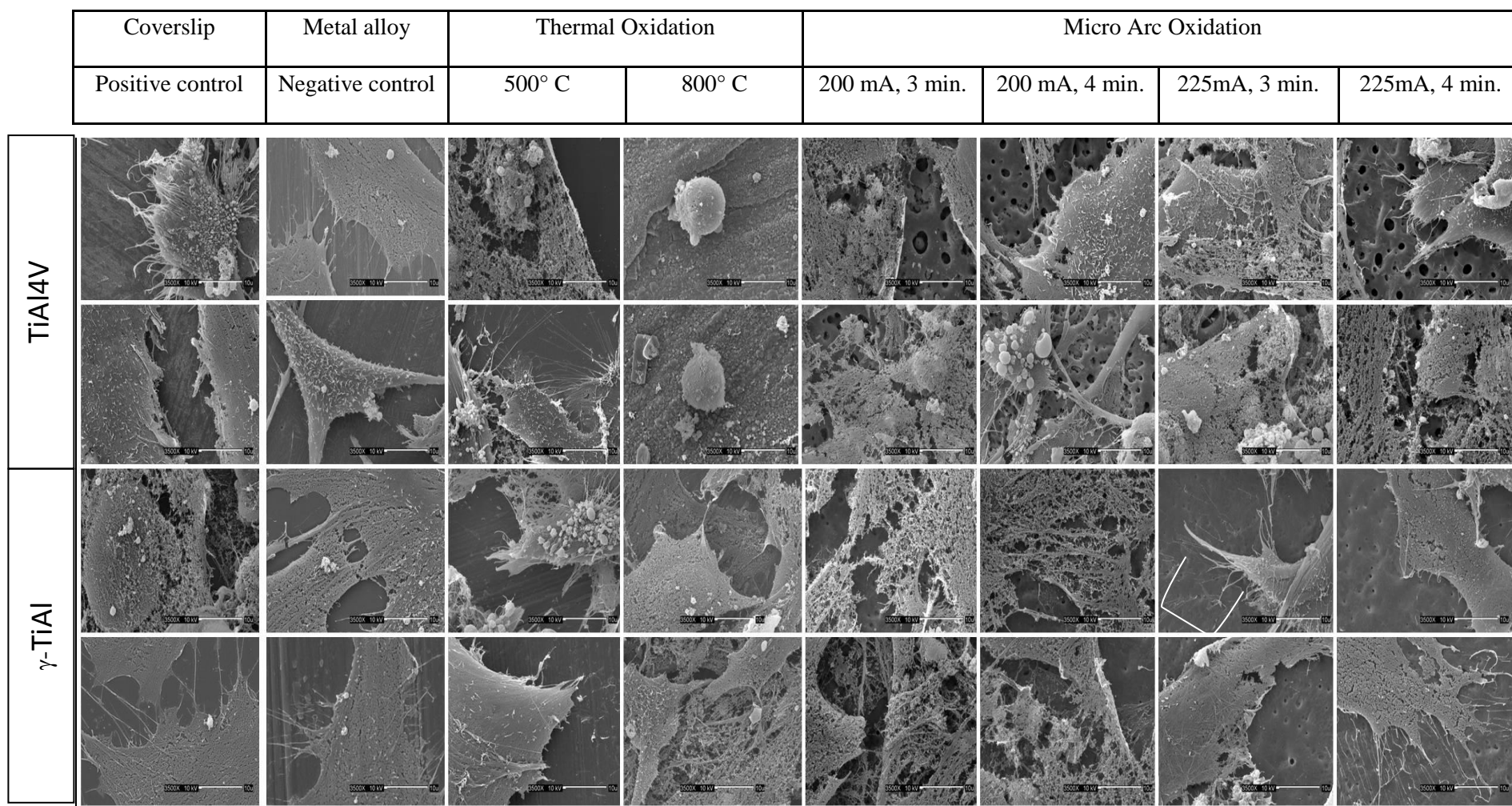
Figure 18: SEM micrographs of hFOB 1.19 cells seeded on a glass coverslip (positive control), GTi and TiV (negative controls), TiV5 and GTi5 (500°C), TiV8 and GTi8 (800°C), MAOTiV (200mA and 225mA at 3 min and 4 min), MAOGTi (200mA and 225mA at 3 min and 4 min) disks and incubated for 10 days (3 days at 33.5ºC and subsequently 7 days at 39.5ºC). Each column shows the cell appearance by SEM on each surface at the magnification of 3500X. The inverted round bracket represents a mitotic like structure (Scale bar: left and center 10µm, right 1µm).

46

	Coverslip	Metal alloy	Thermal Oxidation		Micro Arc Oxidation			
	Positive control	Negative control	500° C	800° C	200 mA, 3 min.	200 mA, 4 min.	225mA, 3 min.	225mA, 4 min.
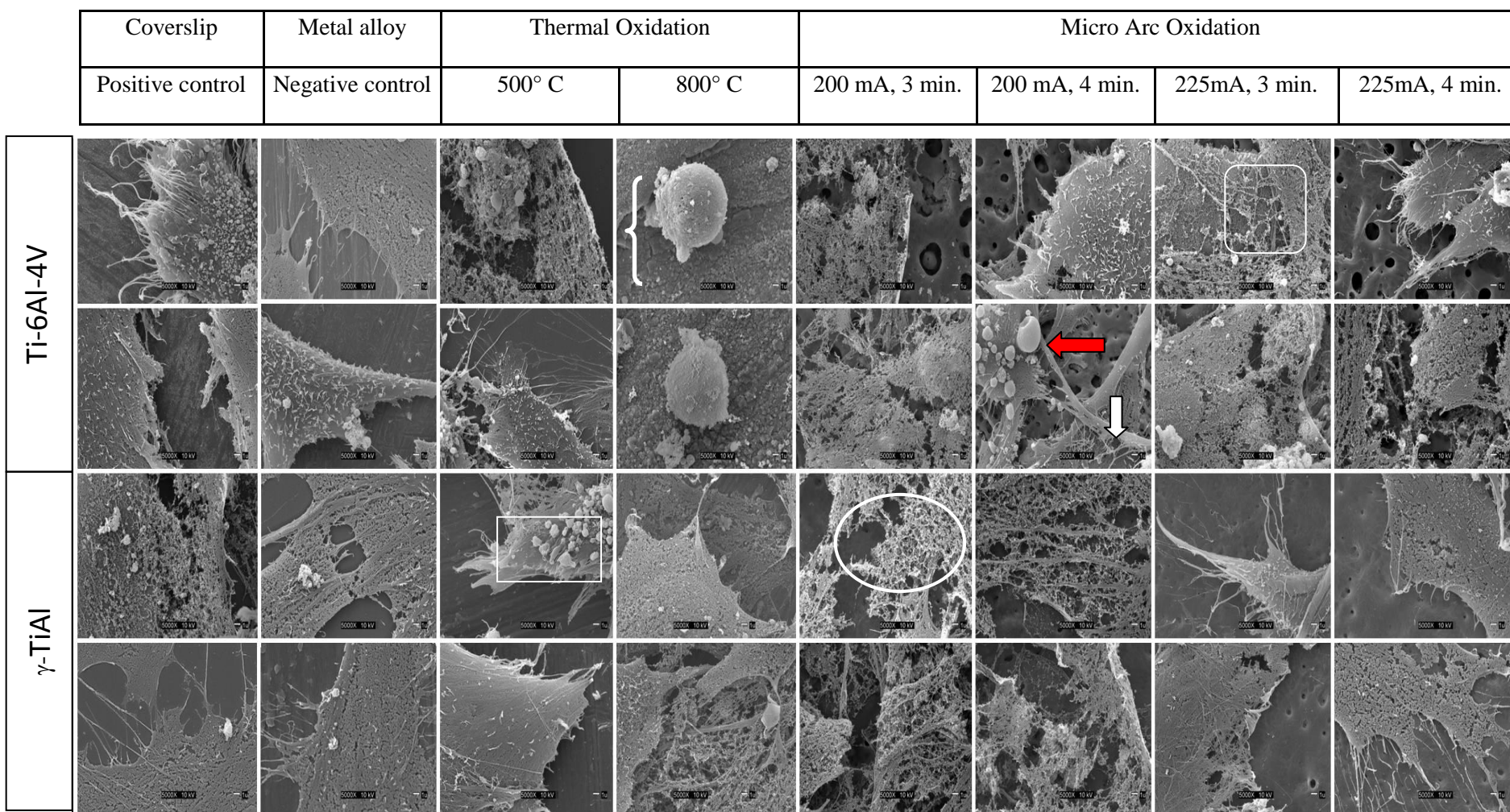
Figure 19: SEM micrographs of hFOB 1.19 cells seeded on a glass coverslip (positive control), GTi and TiV (negative controls) TiV5 and GTi5 (500°C), TiV8 and GTi8 (800°C), MAOTiV (200mA and 225mA at 3 min and 4 min), MAOGTi (200mA and 225mA at 3 min and 4 min) disks. Each column shows the cell appearance by SEM on each surface at the magnification of 5000X. The red arrow represents an elongated cell with mineralized nodule formation. The white arrow indicates filopodia extensions. The white bracket represents an apoptotic cell. The white oval represents the fibrillar network present. The white rectangle represents a fibrous network and mineralized nodules. The rounded square represents the absence of cellular boundaries. (Scale bar: left and center 10μm, right 1μm).

47

6.3 Alkaline Phosphatase Assay

Human osteoblast cell differentiation was evaluated on micro arc oxidized and thermally oxidized Ti-6Al-4V and γ-TiAl surfaces in order to determine their biocompatibility, and possible use as a biomaterial for orthopedic applications. In this research, the ability of the human fetal osteoblast-like cells (hFOB 1.19 cell line) to adhere and differentiate on micro arc and thermally oxidized [500°C (GTi5, TiV5) and 800°C (GTi8, TiV8)] γ-TiAl and Ti-6Al-4V disks respectively, was evaluated both quantitatively and qualitatively. Alkaline Phosphatase Activity was used to quantitatively assess cell differentiation on the different surfaces tested whereas Scanning Electron Microscopy (SEM) was used to qualitatively assess cell adhesion.

In the present study, human osteoblast adhesion on MAOGTi, MAOTiV, GTi5, TiV5, GTi8, and TiV8 surfaces was evaluated at 10 days post-seeding using the alkaline phosphatase assay. Standard curves were used to extrapolate the values of alkaline phosphatase activity on experimental disks based on the alkaline phosphatase assay. Three standard curves were prepared, one for each of the three independent alkaline phosphatase experiments performed in this study. Approximately, 50,000 viable human fetal osteoblasts of the cell line hFOB 1.19, were seeded in 48-well polystyrene plates and incubated for 3 days at 33.5 °C and subsequently 7 days at 39.5°C. There was a linear relationship between the alkaline phosphatase activity in the three standard curves (r^2= 0.9986, 0.9788, and 0.9895) for experimental replicates 1, 2, and 3, respectively. (Appendix B: A and B).

These results suggest that the cells initially attached and proliferated on all the surfaces except TiV8 and the negative controls although cell differentiation was favored on micro arc oxidized alloys. This result was expected, since the hFOB 1.19 cells were incubated until day 3 at a permissive temperature (33.5ºC). Then the samples were changed to a restrictive temperature (39.5ºC) for 7 additional days. At permissive temperatures or at subconfluent cultures, hFOB 1.19 cells exhibit rapid cell division whereas at restrictive temperatures or at confluence, the hFOB 1.19 cell division is slowed down and differentiation increases. This particular behavior of the human fetal osteoblast cell line 1.19 (hFOB 1.19) is due to the presence in its genome of a transfected gene coding for a temperature sensitive mutant (tsA58) of the SV40 T antigen [6]. Expression of T antigen in human cells results in an increased rate of proliferation when it

interacts with the retinoblastoma gene product Rb. Under conditional immortalization, the mutant T antigen is only active (immortalizes cells) at the permissive temperature. Thus, the return to a nonimmortalized state can be manipulated by changing the incubation of the cells to a restrictive temperature [6].

Furthermore, the profile of ALP activity for cells on porous scaffolds is typical during the early stages of differentiation. As ALP activity increases, a drop in activity momentarily occurs coinciding with the initiation of the mineralization process [21]. Zheng *et.al.,* [81] proposed that BMP-2 controls alkaline phosphatase expression and osteoblast mineralization by a Wnt autocrine loop in mesenchymal cells. Mesenchymal stem cells (MSCs) are a heterogenous mixture of cells found in adult bone marrow stroma. MSCs are characterized by their ability to replicate as undifferentiated cells and by their potential to differentiate to several lineages of mesenchymal tissues, including bone, cartilage, fat, and muscle. Among the factors that regulate MSC growth and differentiation are soluble factors and cell–substrate interactions. Although little is known about the molecular mechanisms by which soluble and substrate signals regulate MSC function. They recently showed that the commitment of human MSCs to the osteogenic and adipogenic lineages *in vitro* involves signaling by mitogen-activated protein kinase (MAPK) pathways. In particular, they found that dexamethasone, ascorbic acid, and b-glycerophosphate induce MSC differentiation by regulated the extracellular signal-regulated kinase (ERK1/2) cascade. Furthermore, blocking the ERK1/2 pathway inhibits osteogenic differentiation of MSCs and leads to adipogenesis. Thus MAPK pathways, which are generally activated by growth factors/cytokines and integrin-mediated cell adhesion play a critical role in directing MSC commitment. MAPK pathways are also activated by physical stimuli to regulate the function of a variety of cell types, including bone cells. In bone, it has been proposed that mature cells such as osteocytes and osteoblasts are responsible for sensing and responding to mechanical stimuli [62]. Whether the progenitors that give rise to these cells are responsive to mechanical signals and if so, by what mechanisms remain unknown.

There were no significant differences in the number of osteoblast cells attached on the micro arc oxidized or thermally oxidized surfaces collectively. However, the alkaline phosphatase activity was significantly higher on the cell cultures that grew on the micro arc oxidized alloys than on the thermally oxidized surfaces. Specifically, alkaline phosphatase

activity was significantly higher on the micro arc oxidized γ-TiAl alloys treated at 225mA, with time of exposure of 4 minutes [Table 4 and 5]. The ALP activity on TiV8 was significantly lower than on the other surfaces tested (MAOGTi, MAOTiV, Gti5, TiV5, and Gti8) after 10 days of incubation. Also, ALP activity was significatively lower on the negative controls tested (TiV, Gti).These results suggest that the titanium oxide of the surface of these alloys may be correlated to the differentiation of the osteoblasts. It was demonstrated that the micro arc oxidized alloys consists of titanium oxide with peaks for both anatase and rutile phases in all the coating conditions applied in this study. Both anatase and rutile have been shown to be beneficial in order to enhance nucleation and subsequent hydroxyapatite (HA) precipitation, thereby increasing bioactivity of the titanium surface [54]. Also, it was demonstrated that titanium oxide, particularly in the anatase form, is a photocatalyst under ultraviolet (UV) light. Recently it has been found that titanium oxide, when spiked with nitrogen ions or doped with metal oxide like tungsten trioxide, is also a photocatalyst under either visible or UV light. It also has the potential to oxidize water to create hydroxyl radicals and oxygen or organic materials directly. Therefore, maybe the exposure to ultraviolet light (sterilization used on all alloys in this study to undergo experimentation) has an effect on the composition of the titanium oxide. This may explain the poor cell differentiation observed on the Ti-6Al-4V and γ-TiAl alloys without treatment. Other molecular research suggests that cell cytotoxicity due to TiO_2 results from the interaction between TiO_2 nanoparticles and the lysosomal compartment, independently of the known apoptotic signalling pathways. However, these still has not been fully studied. These results also suggest that that the incorporation of calcium and phosphate to the titanium oxide favor cell differentiation, however the osteoblasts do not depend solely on these ions but more so on the composition of the titanium oxide (observed with the very poor osteoblast differentiation on the negative controls of Ti-6Al-4V and γ-TiAl alloys). Therefore, more studies are needed to determine the direct effects of the titanium oxide on hFOB 1.19 cells.

This particular behavior of hFOB 1.19 cells on TiV8 and the negative controls was the cause of the significant interactions observed between the factors tested (type of metal and treatment) and when the data of the alkaline phosphatase assay was analyzed by an ANOVA [Appendix B, C and D].

The average number of alkaline phosphatase activity and standard deviation (S.D.) of osteoblast cells attached on the micro arc oxidized alloys are shown in Figures 20 through 23 The interaction between the type of metal (γ-TiAl or Ti-6Al-4V), and surface treatment (micro arc oxidation at 200mA-3min, 200mA-4min, 225mA-3min and 225mA-4min; and thermally oxidized at 500°C or 800°C) was significant ($p < 0.05$). There were significant differences in the amount of alkaline phosphatase detected among the six surfaces studied after 10 days of incubation at 33.5°C and 39.5°C, respectively. (Appendix A). The number of osteoblast cells attached to Ti-6Al-4V at 800°C was significantly less compared to the other surfaces. (Appendix B). Additionally, alkaline phosphatase activity was less on the positive control (glass coverslips) and negative controls (metal alloys) in comparison with the micro arc and thermally oxidized alloys.

The factorial ANOVA carried out with the optical density and alkaline phosphatase activity data showed that the interaction between the two factors (type of metal and type of treatment: micro arc oxidation and thermal oxidation) yielded significant differences. In addition, alkaline phosphatase activity increased in γ-TiAl alloys and in treatments that were exposed longer to current density (225mA-3min. and 225mA-4min.). In comparison, Ti-6Al-4V alloys treated with micro arc and thermal oxidation showed a decrease in alkaline phosphatase activity. This may be correlated with the size of the pore diameter of each alloy (demonstrated with SEM). Vasilescu *et.al.,* [70] indicated that high porosities in substrates results in greater bone ingrowths *in vivo* but in a lower mechanical strength; therefore it is suggested that the porosity of the scaffold must be small enough to maintain its mechanical integrity and large enough to provide optimal bioactivity. Therefore, porosity of the substrate may affect cell adhesion and biocompatibility.

A Standard curve was obtained to determine the pNPP concentration [21]. An equation (see section 5.1) to determine alkaline phosphatase activity was used.

Table 4: Average Optical Density and Alkaline Phosphatase Activity of hFOB 1.19 cell line on Ti-6Al-4V alloys.

Treatment	Optical Density (Average)	Alkaline phosphatase activity (Average)
Coverslips (+ control)	0.756	0.0788
200mA,3min.	0.861	0.090
200mA,4min.	1.078	0.112
225mA,3min.	1.125	0.117
225mA,4min.	1.330	0.139
500°C	0.843	0.088
800°C	0.225	0.023
Ti-6Al-4V alloy (negative control)	0.002	0.0002

Table 5: Average Optical Density and Alkaline Phosphatase Activity of hFOB 1.19 cell line on γ-TiAl alloys.

Treatment	Optical Density (Average)	Alkaline phosphatase activity (Average)
Coverslips (+ control)	0.841	0.088
200mA,3min.	1.091	0.114
200mA.4min.	1.210	0.126
225mA,3min.	1.270	0.132
225mA,4min.	1.318	0.137
500°C	0.932	0.097
800°C	0.569	0.059
γ-TiAl alloy (negative control)	0.004	0.0004

Table 4 and 5: Each value represents the mean ± S.D. of three independent experiments, each performed in triplicate.
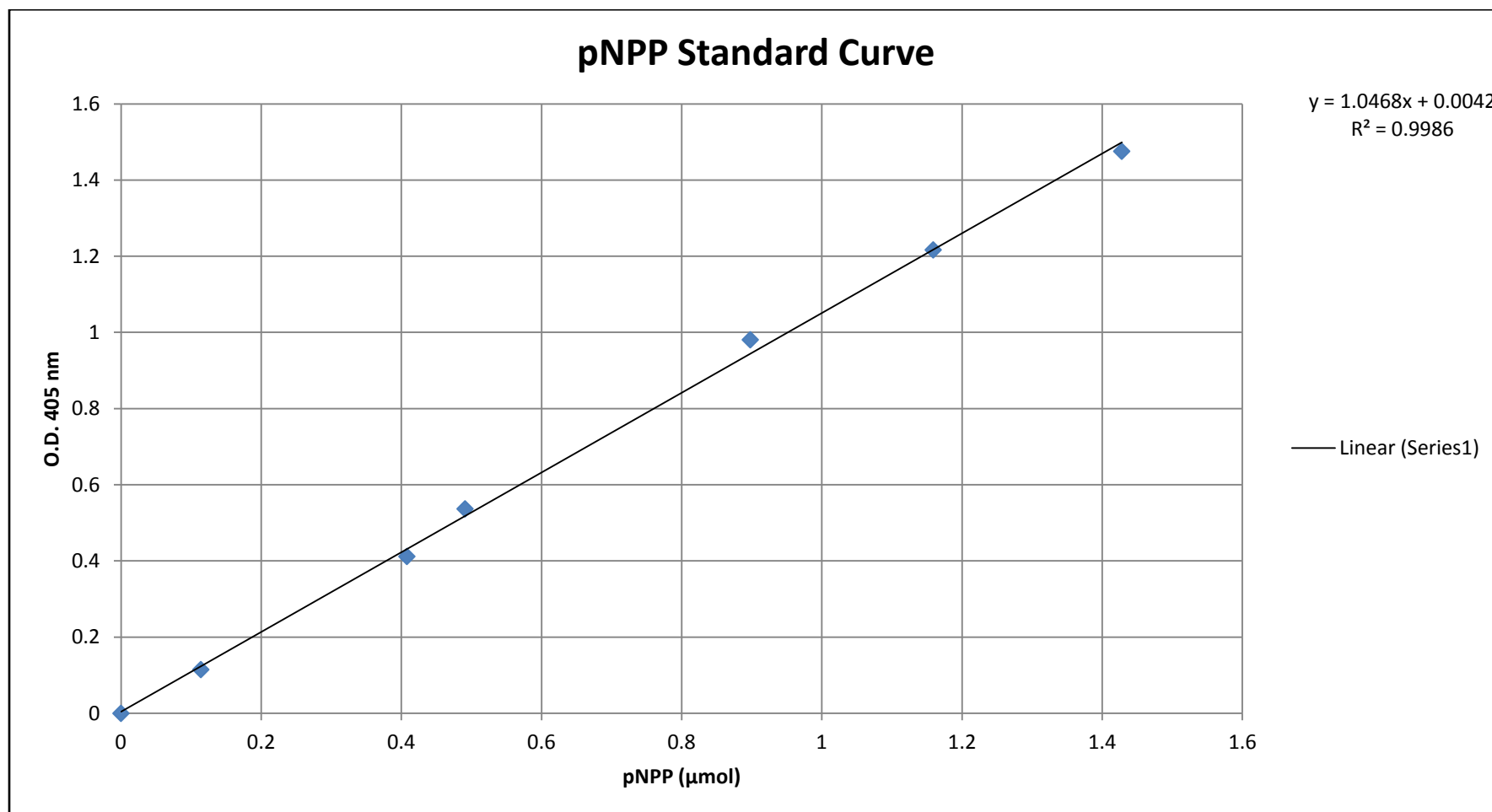
Figure 20: pNPP Standard curve used to extrapolate pNPP concentration to determine ALP activity.
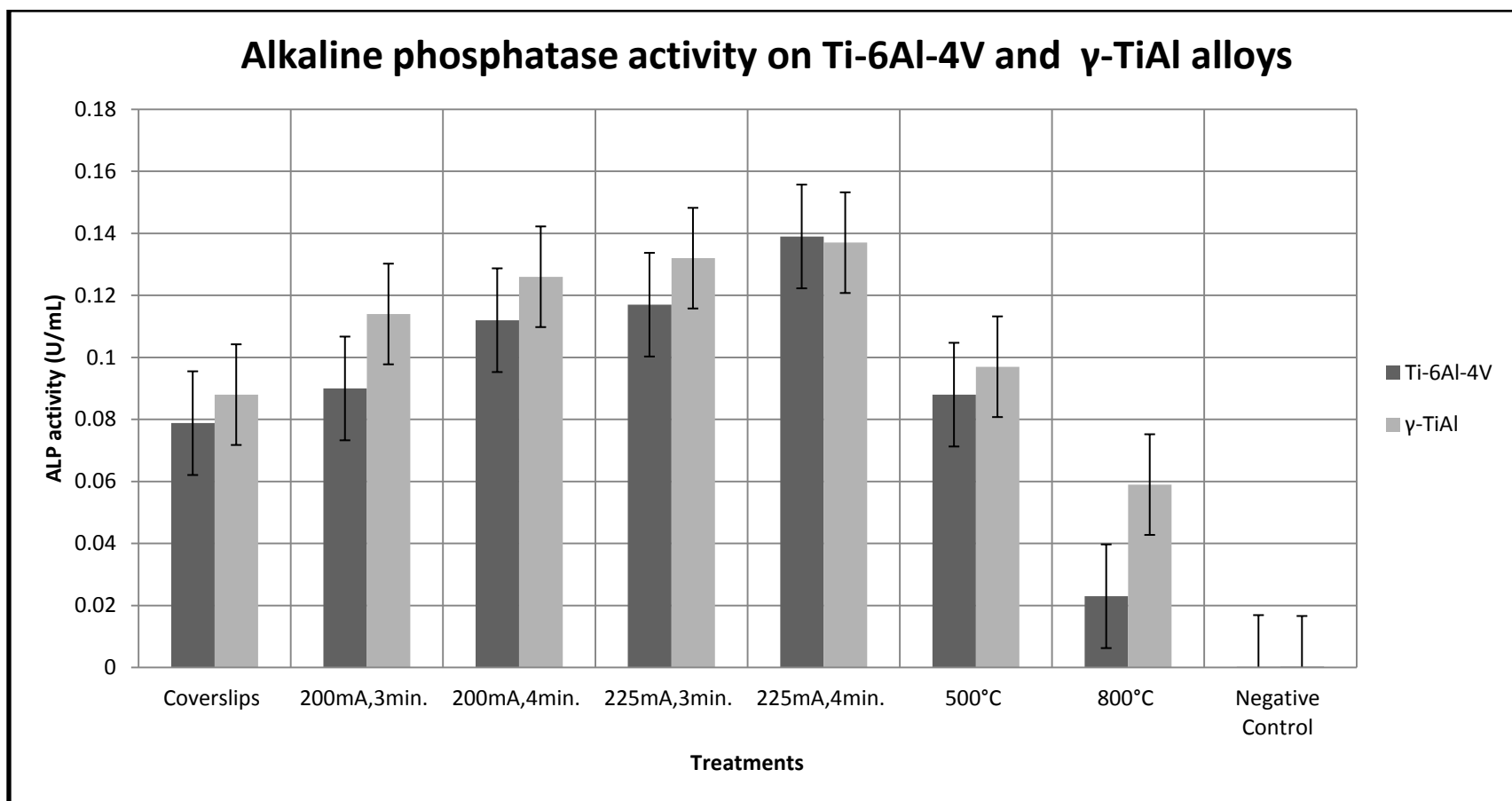
Figure 21: Alkaline phosphatase activity on Ti-6Al-4V and γ-TiAl alloys.
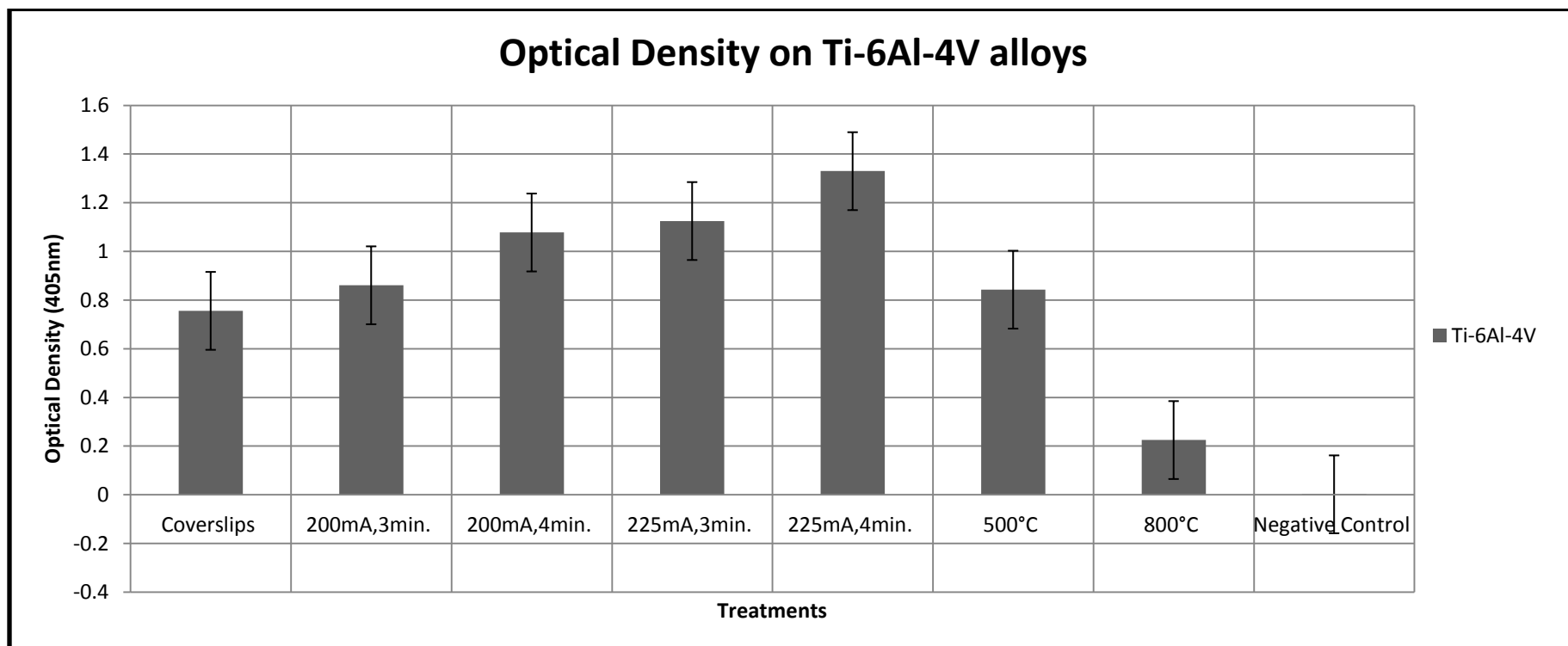
Figure 22: Average Optical Density on Ti-6Al-4Valloys
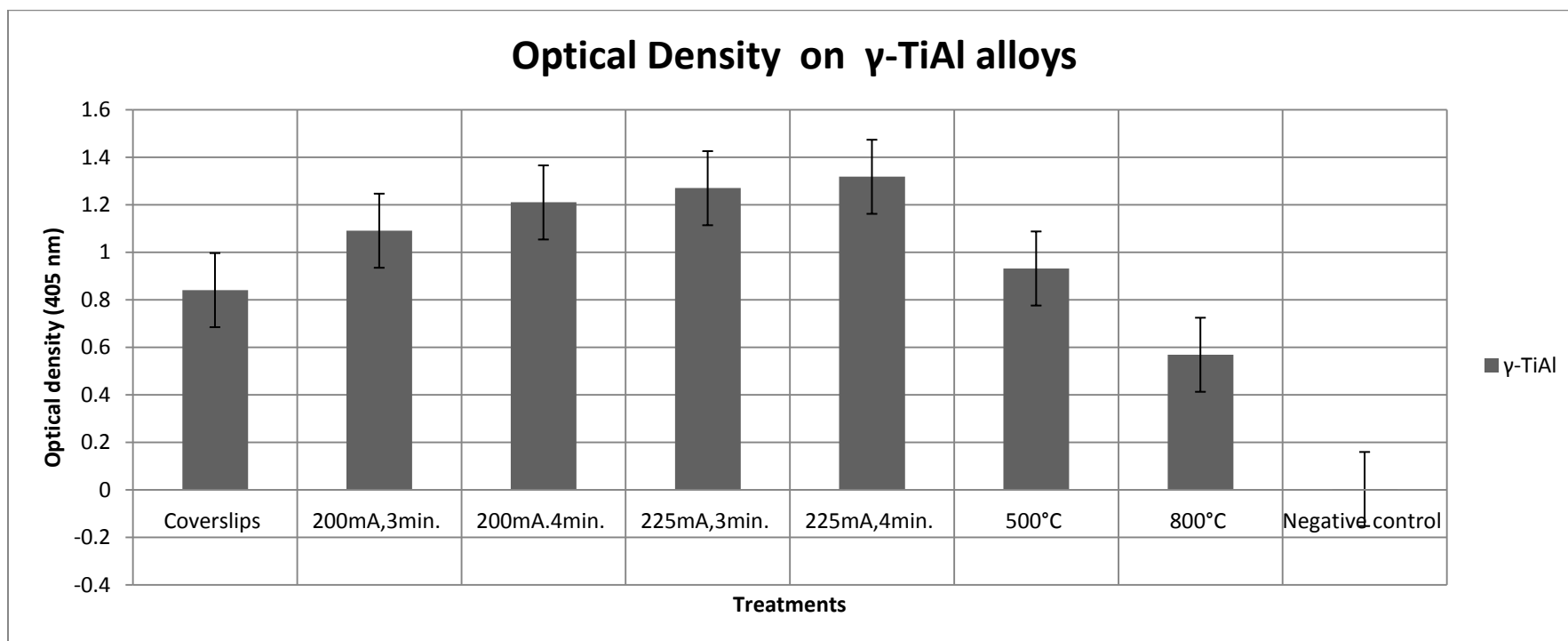
Figure 23: Optical Density on γ-TiAl alloys

6.4 Atomic Force Microscopy (AFM)

Topographical features of the coatings obtained in γ-TiAl and Ti-6Al-4V alloys were analyzed using AFM. The great increase in surface area is noticeable [Figure 24] for the coatings obtained by the MAO method on both alloys. This is a desirable feature especially in hard tissue and structural applications since rough surfaces and highly porous coatings can enable bone osseointegration, producing lasting mechanical interlocking between the implant and bone, thus increasing service life of the implant [40]. Park *et al.,*[54] reported similar results on commercially pure titanium samples subjected to MAO in different electrolytes, and the effect on other surface properties (morphology, composition, etc) was also demonstrated.

For Ti-6Al-4V coatings, the surface area appears to be greater when compared with similar values for γ-TiAl. Roughness measurements were taken in order to correlate these AFM results with quantitative values. The pore diameter was measured for each experimental condition using Image J software. In Ti-6Al-4V alloys, average roughness was greater in thermally oxidized alloys at 800°C , however, this was not taken into consideration due to the cell morphology observed by SEM, where only apoptotic cells were observed. Therefore, cell differentiation could not be directly linked to the average roughness of this surface treatment. The average roughness was greater for the highest current density and time of treatment in Ti-6Al-4V and γ-TiAl alloys treated with micro arc oxidation (225mA, 4 minutes of treatment). However, pore diameter was greatest in Ti-6Al-4V and γ-TiAl alloys without treatment. This is due to the spacing between the atoms that compose the passive oxide present on these alloys. The pore diameter was lower in micro arc oxidized Ti-6Al-4V and γ-TiAl alloys treated at 225mA with 3 minutes of treatment. This may indicate that higher amperage applied on these alloys affect the pore diameter of the oxide. This average roughness and pore diameter may indicate that cells are able to discriminate among subtle differences in surface roughness [18]. Osteoblast cells, not only can discriminate between surfaces of different roughness, but also can discriminate between surfaces with comparable roughness but different topographies. Also, this correlates with the fact that the osteoblasts demonstrated more differentiation on the micro arc oxidized alloys with more amperage and time of treatment since it is suspected that these cells favor smaller pores or diameters that are of a nano scale in comparison to a micro scale.

Therefore, the osteoblasts respond favorable to the nanotopography of the substrates used in this study.

The results summarized in Table 7 correspond to the average value obtained of three replicates of fourteen pore diameter measurements in each sample. Table 6 summarizes these roughness measurements.
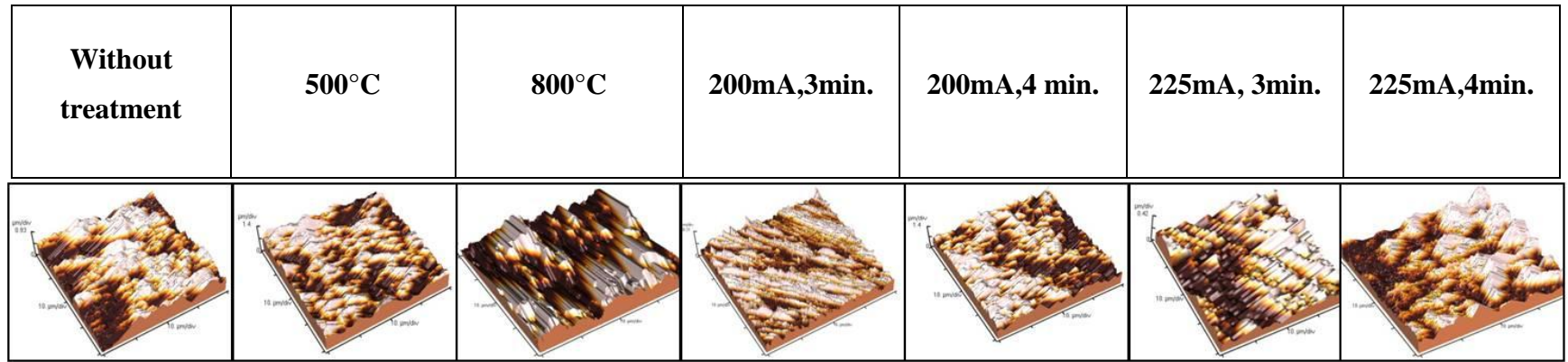
	Without treatment	500°C	800°C	200mA,3min.	200mA,4 min.	225mA, 3min.	225mA,4min.
Ti-6Al-4V							
	a.r: 51.74 p.s: 1.90 o.d: 0.002	a.r: 102.4 p.s: 0 o.d: 0.843	a.r: 318.8 p.s: 0 o.d: 0.225	a.r: 246.3 p.s: 1.59 o.d: 0.861	a.r: 247.6 p.s: 1.80 o.d: 1.078	a.r: 213.3 p.s: 1.48 o.d:1.125	a.r: 301.7 p.s: 1.52 o.d: 1.330
γ-TiAl							
	a.r: 49.30 p.s: 0. 65 o.d: 0.004	a.r: 31.34 p.s: 0 o.d: 0.932	a.r: 65.88 p.s: 0 o.d: 0.569	a.r: 174.5 p.s: 0.49 o.d: 1.091	a.r: 185.9 p.s: 0.52 o.d: 1.210	a.r: 137.5 p.s: 0.37 o.d: 1.270	a.r: 189.8 p.s: 0.44 o.d: 1.318
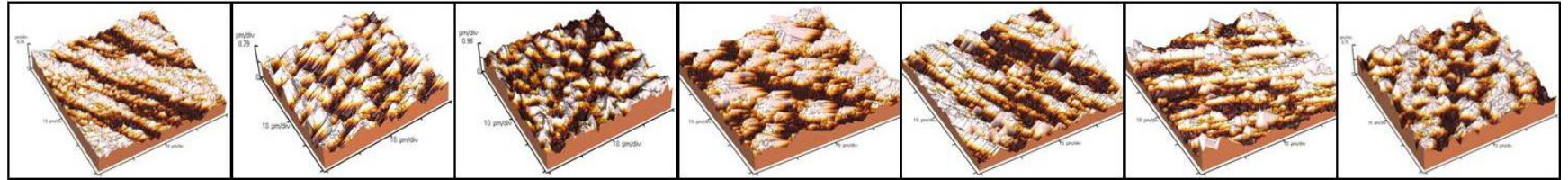
Figure 24: Morphological characterization of micro oxidized Ti-6Al-4V and γ-TiAl alloys by AFM. Each column shows the surface appearance by Atomic Force Microscopy at each treatment (without treatment, 500°C, 800°C, 200mA at 3 and 4 minutes, and 225mA at 3 min and 4 minutes of treatment) respectively. Average roughness (a.r) is represented in nanometers (nm) and pore size (p.s) is represented in micrometers (μm). Optical density is referred to as (o.d).

Table 6: Average roughness measurements for Micro Arc Oxidized treated γ-TiAl and Ti-6Al-4V alloys by Atomic Force Microscopy.

Ti-6Al-4V	Average roughness (nm)	γ-TiAl	Average roughness (nm)
without treatment	51.74	without treatment	49.30
200mA,3min.	246.3	200mA,3min.	174.5
200mA,4min.	247.6	200mA,4min.	185.9
225mA,3min.	213.3	225mA,3min.	137.5
225mA,4min.	301.7	225mA,4min.	189.8
500°C	102.4	500°C	31.34
800°C	318.8	800°C	65.88

Table 7: Average pore diameter measurements for Micro Arc Oxidized treated γ-TiAl and Ti-6Al-4V alloys by Image J.

Ti-6Al-4V	Average pore diameter (μm)	γ-TiAl	Average pore diameter (μm)
without treatment	1.90	without treatment	0.65
200mA,3min.	1.59	200mA,3min.	0.49
200mA,4min.	1.80	200mA,4min.	0.52
225mA,3min.	1.48	225mA,3min.	0.37
225mA,4min.	1.52	225mA,4min.	0.44
500°C	0	500°C	0
800°C	0	800°C	0

6.5 Effects of Surface Topography on cellular adhesion and differentiation

As established earlier by compositional and morphological analysis of the MAO coatings, the properties of the oxide coating are strongly dependent on the process parameters used, and are also material specific for each titanium alloy. Therefore, *in vitro* studies on cell attachment (demonstrated qualitatively with SEM), proliferation and differentiation (demonstrated quantitatively with ALP) were concerned with the influence of surface topography (demonstrated quantitatively with AFM).

Many investigators have examined the effects of surface topography (porosity) on bone ingrowth in porous metals using *in vivo* models [69]. While a range of pore sizes has been identified within which bone ingrowth occurs, no consensus on optimal pore size exists due to the range of materials investigated and their respective microstructural impacts. Similar *in vitro* studies indicate that pore size is an important microstructural parameter in the design of three-dimensional osteoconductive scaffolds [68].

Cell attachment proteins (fibronectin and vitronectin) adhere to the surface depending on the amount of calcium ions present on the titanium substrate. Calcium and phosphate ions are suggested to enhance any initial response *in vitro* due to their high content in bone [47]. The results suggest that calcium and phosphate ions on the surface lead to the stronger absorption ability of proteins and osteoblast ligands. Thus the initial cell adhesion (measured qualitatively by SEM) is considered chemical rather than physical. In addition, calcium ions mediate cell-cell communication via gap junctions. The dissolution of calcium ions on the surface containing calcium increased ion concentration might also be beneficial to cell adhesion and higher cell activity. Kim *et al.,* [37] reported that the formation of a bone like structure on titanium alloys was a multi step process involving absorption of calcium ions, then the absorption of phosphate ions, and then the formation of amorphous calcium phosphate, and the final transformation into the apatite layer. This multi step process is considered to have mayor impact in the osseointegration of titianium alloys.

In addition, cell differentiation is essential to provide osseointegration because it indicates a high presence of the alkaline phosphatase enzyme (ALP). ALP is among the first functional genes expressed in the process of calcification. It is therefore likely that at least one of

its roles in the mineralization process occurs at an early step. A clue to the role of ALP in calcification came from studies of hypophosphatasia patients, whose disease results from missense mutations in the gene coding for TNAP leading to decreased or absent ALP activity. ALP is a cell surface glycoprotein that is involved with mineralization. Osteopontin and Bone sialoprotein (BSP) are secreted, bind cell surface integrin receptors, and regulate mineralization. Osteocalcin is a matrix protein that regulates osteoclast activity. Biglycan is a small leucine-rich proteoglycan binds to various extracellular matrix components and has a role in mineralization. Expression of each of these markers is detected at a specific stage of osteogenic maturation. For instance, the expression of ALP is acquired during early differentiation. Osteopontin is expressed throughout matrix maturation, followed first by BSP and, finally, by osteocalcin, which characterizes the post-proliferate phase [3]. Biglycan is expressed relatively early during matrix assembly and acts to regulate organization of the extracellular matrix [4]. ALP activity was studied by Marom *et.al.,* [49], which showed an increase in activity with increasing cell density and time in culture. Apart from ALP, osteopontin and osteocalcin showed an increase in staining intensity as a function of cell density. Different studies elaborated on the importance of these matrix proteins in matrix mineralization [26].

Osteogenic cells require an interaction with the extracellular matrix for their growth, maturation, and survival. Collagen I is the predominant protein of bone matrix, and its expression and secretion is critical for mineralization process. Attachment to collagen I is mediated through integrins that activate kinase signaling pathways, thus supporting osteoblast cell proliferation and bone growth [7,24,48,50]. The role of various matrices such as collagen I, osteopontin, and osteonectin on growth and differentiation of marrow stromal cells was studied at the level of changes in cell morphology, gene expression, and enzymatic activities [47]. The results presented in this study indicate that MBA-15 cells can attach and spread on a collagenous matrix, but not on BSA. Lack of attachment-mediated signals may result in diminished survival and lead to cell death as measured by intracellular Ca levels.

Therefore, the rugosity and porosity of the surface is of significant importance. Cells are able to discriminate among subtle differences in surface roughness [18]. Osteoblast-like cells can discriminate not only between surfaces of different roughness but also between surfaces with comparable roughness but different topographies [13]. However, factors and mechanisms

underlying the response of cells in contact with Ti alloys are poorly understood. For example, cells cultured on cpTi and Ti alloys display differential response, although both surfaces are covered with TiO2 [2]. Thus, these differences could be attributed to the microstructure, crystallinity or chemistry of the substrate.

In conclusion, numerous variables influence the biocompatibility and osteogenic potency of nanostructured biomaterials *in vitro* and *in vivo*. The surface structure and the composition of a biomaterial affect cellular attachment, adherence, proliferation and migration, and also differentiation and survival of defined cell types. Chemical composition, surface structure (topography, geometry, roughness, particle size), surface energy, hydrophobicity, and the degree of solubility in aqueous solutions of a biomaterial will define an implant concerning its osteblast promoting potency.

Conclusions

- Micro arc oxidation treatment was successfully applied on Ti-6Al-4V and γ-TiAl alloys to generate porous and thick, multilayered coatings.

- The surface of materials studied with deposited calcium and phosphorous ions (MAO treatment) were favorable for cell proliferation and differentiation. hFOB 1.19 cells were capable of attaching and spreading on both micro arc oxidized and thermally oxidized Ti-6Al-4V and γ-TiAl alloys.

- The alkaline phosphatase assay performed after 10 days of incubation, demonstrated that hFOB 1.19 cells were able to differentiate on the different surfaces tested. However, the number of cells attached on Ti-6Al-4V thermally oxidized at 800°C and the negative controls (Ti-6Al-4V, γ-TiAl), were significantly less compared to the number of cells attached on the other surfaces evaluated, at 10 days post seeding. Results suggest that all tested surfaces but TiV8 and the negative controls are biocompatible.

- SEM analyses did not show apparent differences in the morphology of hFOB cells cultured on the different surfaces tested after 10 days, respectively.

- Micro arc oxidized surfaces (at 200mA and 225mA at 3 and 4 minutes, respectively) allowed hFOB 1.19 cell adhesion and differentiation. No apparent cytotoxic effects were observed on hFOB 1.19 cells, suggesting that these surfaces have the potential to be used as implant materials.

- Cell differentiation was minimized with the presence of a passive titanium oxide in comparison to micro arc oxidized and thermally oxidized Ti-6Al-4V and γ-TiAl alloys. Therefore, the presence and type of titanium oxide has a direct impact on osteoblast adhesion and differentiation.

Recommendations

To further validate micro arc oxidation as a biomaterial the following studies are recommended:

1. Evaluate the wear resistance *in vitro* of all micro arc oxidized treated surfaces to determine whether they are possibly good candidates for *in vivo* studies.

2. Modify the MAO treated surfaces with the application of hydroxyapatite to further enhance biocompatibility.

3. Measure the gap between the cell layer and metal surface to determine interfacial adhesion between osteoblasts and substrate.

4. Study calcium composition of hFOB 1.19 osteoblast cells cultured on micro arc oxidized γ-TiAl and Ti-6Al-4V alloys using alizarin red staining. The presence of calcium in the samples can serve as a marker for normal bone formation.

5. Perform an immunofluorescent assay to determine cell adhesion markers (vinculin) with actin-F on the micro arc oxidized surfaces to determine the formation and maturation of focal adhesions points on the different surfaces.

6. *In vivo* studies should be performed in order to establish the use of micro arc oxidized and thermally oxidized γ-TiAl alloys as implants.

7. Evaluate solely the use of titanium oxide to determine its effects on cell adhesion and differentiation.

Literature Cited

[1] Advincula M.C., Rahemtulla F.G., Advincula R.C., Ada E.T., Lemons J.E., Bellis S.L. 2006. Osteoblast adhesion and matrix mineralization on sol-gel-derived titanium oxide. Biomaterials. Apr;27(10):2201-12. Epub 2005 Nov 28.

[2] Anselme, K. 2000. Osteoblast adhesion on biomaterials. Biomaterials 21: 667-681.

[3] Aubin, J.E. 2001. Regulation of osteoblast formation and function. Rev Endocrine Metabolic Disorder Jan;2(1):81-94.

[4]Balint R., A. Rupani, S. Cartmell, 2012.Osteoblasts and their applications in bone tissue engineering. Cell Health and Cytoskeleton. May 2012; 4. 49-61.

[5] Barthlott W., C. Neinhuis. 1997. Purity of the sacred lotus, or escape from contaminations in biological surfaces. Planta 202: 1-8.

[6] Bello-Melo, S. 2009. Effects of thermal oxidation of γ titanium aluminide on human osteoblast adhesion. M.S.Thesis, University of Puerto Rico, Mayaguez.

[7] Carvalho R., P. Kostenuik, E. Salih, A. Bumann, L. Gerstenfeld. 2003. Selective adhesion of osteoblastic cells to different integrin ligands induces osteopontin gene expression. Matrix Biol 22(3):241–249.

[8] Castañeda, D.F. 2003. Evaluation of γ -TiAl as an Implant Material. M. S.Thesis, University of Puerto Rico, Mayagüez.

[9]. Castañeda-Muñoz, D.F., P.A. Sundaram, N. Ramírez. 2007. Bone tissue reaction to Ti-48Al-2Cr-2Nb (at.%) in a rodent model: a preliminary SEM study. J Mater Sci Mater Med. 18 (7):1433-8.

[10] Ceschini L., E. Lanzoni, C. Martini, D. Prandstaller, G. Sambogna. 2008. Comparison of dry sliding friction and wear of Ti-6Al-4V alloy treated by plasma electrolytic oxidation and PVD coating. Wear;264: 86-95

[11] Cooper L.F. 2000. A role for surface topography in creating and maintaining bone at titanium endosseous implants. J Prosthet Dent 84: 522-534.

[12] Cullinane D.M, T.A. Einhorn. 2002. Biomechanics of bone. In: Bilezikian JP, Raisz LG, Rodan GA, editors. Principles of bone biology. San Diego: Academic Press; p. 17–32.

[13] Curtis A.S.G, M. Varde.1964. Control of cell behaviour: topological factors. J Natl Cancer Inst 33: 15-26.

[14] Curtis A.S.G. and C. Wilkinson. 2001. "Nanotechniques and approaches in biotechnology," *Trends in Biotechnology*, vol. 19,no. 3, pp. 97–101.

[15] Dalby M.J., L. Di Silvio, G.W. Davies and W. Bonfield. 2000 Surface topography and HA filler volume effect on primary human osteoblasts *in vitro* J Mat Sci: Mater Med 11: 805-810.

[16] Davis J.E, B. Lowenberg, A. Shiga. 1990. The bone-titanium interface *in vitro*. J Biomed Mater Res 24:1289-1306.

[17] Delgado-Alvarado, C., P.A. Sundaram. 2006. Corrosion evaluation of Ti-48Al-2Cr-2Nb (at.%) in Ringer's solution. Acta Biomaterialia 2(6): 701-708.

[18] Deligianni, D.D., N.D. Katsala, P.G. Koutsoukos, Y.F. Missirlis. 2001. Effect of surface roughness of hydroxyapatite on human bone marrow cell adhesion, proliferation, differentiation and detachment strength. *Biomaterials*, *22*, 87-96.

[19] Escudero, M.L., Muñoz-Morris M.A., García-Alonso M.C., Fernández-Escalante E., 2004. *In vitro* evaluation of a Taylor Francis: γ-TiAl intermetallic for potential endoprothesic applications. Intermetallics 12: 253-260.

[20] Evgeny A. Z., A. Janiak, J. Hang, A. Waghray, A.M. Belkin. 2006. The role of tissue transglutaminase in cell-matrix interactions. Frontiers in Bioscience 11, 1057-1076.

[21] Fernley, H.N. 1971. The Enzymes (Boyer, P.D., ed.), Vol. IV, 3rd ed; 417-447.

[22] Frauchiger, V., L.C. Baxter. 2002. Fibroblast and osteoblast adhesion and morphology on calcium phosphate surfaces. Eur Cell Mater 4: 1-17.

[23] García-Alonso, M.C., L. Saldaña, G. Vallés, J.L. González-Carrasco, J. González-Cabrero, M.E Martínez, E. Gil-Garay, and L. Munuera. 2003. *In vitro* corrosion behavior and osteoblast response of thermally oxidised Ti-6Al-4V alloy. Biomaterials 24: 19-26.

[24] Geiler, U., U. Hempel, C. Wolf, D. Scharnweber, H. Worch and K.W. Wenzel. 2000. Collagen type I-coating of Ti-6Al-4V promotes adhesion of osteoblasts. J Biomed Mater Res. 51: 752-760.

[25] Gleiche M., L.F. Chi, H. Fuchs. 2000. Nanoscopic channel lattices with controlled anisotropic wetting. Nature 403: 173-175.

[26] Groeneveld E.H, J.P. van den Bergh, P. Holzmann, C.M. ten Bruggenkate, D.B. Tuinzing, E.H. Burger. 1999. Mineralization processes in demineralized bone matrix grafts in human maxillary sinus floor elevations. J Biomedical Materials Res;48(4):393–402.

[27] Guo H.F, M.Z. An, H.B. Huo, S. Xu, L.J Wu. 2006. Microstructure characteristic of ceramic coatings fabricated on magnesium alloys by micro-arc oxidation in alkaline silicate solutions [J]. Applied Surface Science,, 252: 7911−7916.

[28] Han Y, S.H Hong, K. Xu. 2002. Synthesis of nanocrystalline titania films by micro-arc oxidation. Mater Lett; 56:744–7.

[29] Harris, S.A., R. Enger, L. Riggs, T. Spelberg. 1995. Development and characterization of a conditionally immortalized human fetal osteoblastic cell line. J Bone Miner Res, 10(2): 178-186.

[30] Human bone structure. www.nasa.gov [Online]. Available: http://lis.arc.nasa.gov/lis2/Chapter4_Programs/NIH_C/NIH_C1.html [Accessed: 9 January 2013].

[31] Integrin Structure. Source: Frontiers in Bioscience. www.bioscience.org [Online]. Available: http://www.bioscience.org/2006/v11/af/1863/list.htm. Accessed: [9 January 2013]

[32] Ishizawa H, Ogino M. 1995.Formation and characterization of anodic titanium oxide films containing Ca and P. J Biomed Mater Res; 29: 65–72.

[33] Jager M., C. Zilkens, K. Zanger, R. Krauspe. 2007. Significance of Nano and Microtopography for Cell-Surface Interactions in Orthopaedic Implants. Journal of Biomedicine and Biotechnology. Volume 2005; 19 pages.

[34] Jee, W.S.S. 1988. The skeletal tissues. In L. Weiss (ed) 6th ed., Cell and Tissue Biology Urban: Schwarzenberg. Baltimore. , pp. 218-234.

[35] Junqueira, L.C., J. Carneiro. 2003. Basic Histology. Text and Atlas. 10th Ed. Mc Graw Hill Company: New York, pp. 141-148.

[36] Keaveny T.M, E.F. Morgan, G.L Niebur, O.C Yeh. 2001. Biomechanics of trabecular bone. Annu Rev Biomed Eng; 3:307–33.

[37] Kim M.S, J.J Ryu, Y.M Sung. 2007. One-step approach for nano-crystalline hydroxyapatite coating on titanium via micro-arc oxidation. Electrochemistry Community;9:1886–91.

[38] Kurzweg H, R.B Heimann, T. Troczynski. 1998.Development of plasma sprayed bioceramic coatings with bond coats based on titania and zirconia. Biomaterials ;19: 1507–15.

[39] Kwon S.Y, T. Lin, H. Takei, Q. Ma, D.J. Wood, D. O'Connor, K.L. Sung. 2001. Alterations in the adhesion behavior of osteoblasts by titanium particle loading: inhibition of cell function and gene expression. Biorheology, Vol. 38, No. 2-3, pp. 161-83.

[40] Lara-Rodriguez, L. 2010. Electrochemical characterization of plasma electrolytic oxidation coatings on γ-TiAl and Ti-6Al-4V for biomedical applications. M.S.Thesis, University of Puerto Rico, Mayagüez.

[41] Lee S.H, H.W. Kim, E.J. Lee, L.H. Li, H.E. Kim. 2006. Hydroxyapatite-TiO2 coating on Ti implants. J Biomater Appl ;20: 195–208.

[42] Li A., H.W. Kim, S.H. Lee, Y.M. Kong, H.E. Kim. 2005. Biocompatibility of titanium implants modified by micro arc oxidation and hydroxyapatite coating. J Biomed Mater Res;73a:48–54.

[43] Li D., B. Liu, J. Wu and J. Chen. 2001. Bone interface of dental implants cytologically influenced by a modified sandblasted surface: a preliminary *in vitro* study. Implant Dentistry, vol. 10, no. 2, pp. 132–138.

[44] Li J., P. Li, S.H. Li, C.A.Van Blitterswijk and K. de Groot. 2005. A novel porous Ti-6A1-4V: characterization and cell attachment. Journal of Biomedical Materials Research Part A, vol. 73, no. 2, pp. 223–233.

[45] Li L., Y. Kong, H. Won. 2004. Improved biological performance of Ti implants due to surface modification by micro arc oxidation. Biomaterials; 25: 2867-2875.

[46] Lin C.Y., N. Kikuchi and S.J. Hollister. 2004. A novel method for biomaterial scaffold internal architecture design to match bone elastic properties with desired porosity. J Biomech; 37(5):623

[47] Ma PX. Scaffolds for tissue fabrication.2004 Materials Today; 7:30–40.

[48] Marks Jr S.C, P.R. Odgren. 2002. Structure and development of the skeleton. In: Bilezikian JP, Raisz LG, Rodan GA, editors. Principles of bone biology. 2nd ed. San Diego: Academic Press; p. 3–15.

[49] Marom R., I. Shur, R. Solomon, D. Benayahi. 2005. Characterization of Adhesion and Differentiation Markers of Osteogenic Marrow Stromal Cells. Journal of Cellular Physiology. 202:41-48.

[50] Mizuno M., Y. Kuboki. 2001. Osteoblast-related gene expression of bone marrow cells during the osteoblastic differentiation induced by type I collagen. J Biochem (Tokyo) 129(1):133–138.

[51] Muller U., T. Imwinkelried, M. Horst, M. Sievers and U. Graf-Hausner. 2006. Do human osteoblasts grow into open porous titanium? European Cells and Materials, vol. 11, pp.8–15.

[52] Nie J.H, Y.L. Shi, F.Y. Yan, J.Z Chen, L. Wang. 2008.Preparation of hydroxyapatite-containing titania coating on titanium substrate by micro-arc oxidation. Mater Res Bull;43:45–53.

[53] O'Connor D.T, M.G Choi, S.Y. Kwon and K.L. Sung. 2004. New insight into the mechanism of hip prosthesis loosening: effect of titanium debris size on osteoblast function. Journal of Orthopaedic Research, vol. 22, no. 2, pp. 229–236.

[54] Park. J.K. 1984. The effect of surface topography on micro arc oxidized alloys. Biomaterials Science and Engineering. Plenum Pub. Corp. NewYork, London, 1984.

[55] Park K.H, S.J. Heo, J.Y. Koak, S.K. Kim, J.B. Lee and S.H. Kim. 2007.Osseointegration of anodized titanium implants under different current voltages: a rabbit study. J Oral Rehabilitation;34:517–27.

[56] Park, Y.J., K.H. Kim, J.Y. Lee, Y. Ku, S.J. Lee, B.M. Min, C.P. Chung. 2006. Immobilization of bone morphogenetic protein-2 on a nanofibrous chitosan membrane for enhanced guided bone regeneration. Biotechnol. Appl. Biochem. 2006, 43, 17-24.

[57] Pei-bo S.U., W.U. Xiao-hong, G.U. Yun, J. Zhao-hua. 2009. Effects of cathode current density on structure and corrosion resistance of plasma electrolytic oxidation coatings formed on ZK60 Mg alloy [J]. Journal of Alloys and Compounds, 475: 773−777.

[58] Periodic Table of Elements. Source: Frontiers in Bioscience. www.trudeau.hs.yrdsb.edu [Online]. Available: http://www.trudeau.hs.yrdsb.edu.on.ca. Accessed: [9 May 2013]

[59] Piehler, H.R. 2006. Metallic biomaterials. In: S. Guelcher and J. Hollinger (eds.), An introduction to Biomaterials,Taylor Francis: Boca Raton. pp. 291-304.

[60] Qu Z., X. Rausch-Fan, M. Wieland, M. Matejka and A. Schedle. 2007. The initial attachment and subsequent behavior regulation of osteoblasts by dental implant surface modification. Journal of Biomedical Materials Research Part A, vol. 82, no. 3,pp. 658–668.

[61] Rivera-Denizard, O., N. Diffoot-Carlo, V. Navas, P.A. Sundaram. 2008. Biocompatibility studies of human fetal osteoblast cells cultured on γ titanium aluminide. J Mater Sci Mater Med. 19(1): 153-158.

[62] Robey P.G., J.D. Termine.1985. Human Bone Cells *In Vitro*. Calcif. Tissue Int. Sept; 37(5): 454-460.

[63] Ross, M.H., G.I. Kaye, W. Pawlina. 2003. Histology: A Text and Atlas 4th Ed. Lippincott Williams and Wilkins, USA.

[64] Ross, M. and W. Pawlina. 2006. Histology. A text and Atlas. 5th Ed. Lippincott Williams Wilkins: Baltimore, pp. 202-217.

[65] Song H., M.K. Kim, G.C. Jung. 2007. The effects of spark anodizing treatment of pure titanium metals and titanium alloys on corrosion characteristics. Surface and Coatings Technology; 201:8738-45.

[66] Sousa S.R., M.A Barbosa. 1996. Effect of hydroxyapatite thickness on metal ion release from Ti-6Al-4V substrates. Biomaterials; 17:397-404.

[67] Stangl R, A. Pries, B. Loos, M. Müller, R.G. Erben. 2004. Influence of pores created by laser superfinishing on osseointegration of titanium alloy implant J Biomed Mater Res A 2004: pp 444-536.

[68] St-Pierre J.P, M. Gauthier, L.P. Lefebvre and M. Tabrizian. 2005. Three-dimensional growth of differentiating MC3T3-E1 pre-osteoblasts on porous titanium scaffolds. Biomaterials,; 26, 7319–7328.

[69] Subramaniam, M., S.M. Jalal, D.J. Rickard, S.A. Harris, M.E. Bolander, T.C. Spelsberg. 2002. Further characterization of human fetal osteoblastic hFOB 1.19 and hFOB/ER cells: bone formation *in vivo* and karyotype analysis using multicolor fluorescent in situ hybridization. J Cell Biochem, 87: 9-15.

[70] Vasilescu C., J.M. Calderon Moreno and A. Cimpean. 2011. Synthesis, Mechanical and Structural Properties and Biological Activity of some nanostructures bone scaffolds. Digest Journal of Nanomaterials and Biostructures Vol. 6, No 2, April - June 2011, p. 523 – 534.

[71] Vassilis K. and D. Kaplan. 2005. Porosity of 3D biomaterial scaffolds and osteogenesis. Biomaterials 26: 5474–5491.

[72] Wang J.H, C.H. Yao, W.Y. Chuang and Young T.H . 2000. Development of biodegradable polyesterurethane membranes with different surface morphologies for the culture of osteoblasts. J Biomed Mater Res 15: 761-770.

[73] Ward B.C. and T. Webster. 2004. Effect of metal substrate nanometer topography on osteoblast metabolic activities. Biological and Bioinspired Materials and Devices, vol. 823, Materials Research Society, San Francisco, Calif, USA, vol.823: 249–254.

[74] Ward B.C and T. Webster. 2006. The effect of nanotopography on calcium and phosphorus deposition on metallic materials *in vitro*. Biomaterials, vol. 27, no. 16, pp. 3064–3074.

[75] Wei D., Y. Zhou, D. Jia, Y. Wang. 2008.Chemical treatment of TiO2 based coatings formed by plasma electrolytic oxidation in electrolyte containing nano HA, calcium salts and phosphates for biomedical applications. Applied surface science; 254: 1775-1782.

[76] Woo K.M, V.J. Chen, P.X. Ma. 2003. Nano-fibrous scaffolding architecture selectively enhances protein adsorption contributing to cell attachment. J Biomed Mater Res; 67:531−7.

[77] Yao Z., Z. Jiang, F. Wang, G. Hao. 2007. Oxidation behavior of ceramic coatings on Ti-6Al-4V by microplasma oxidation. Journal of materials processing technology;190: 117-122

[78] Yen, M.L., C.C. Chien, I.M. Chiu, H.I. Huang, Y.C. Chen, H.I. Hu, B.L. Yen. 2007. Multilineage differentiation and characterization of the human fetal osteoblastic 1.19 cell line: a possible *in vitro* model of human mesenchimal progenitors. Stem Cells, 25:125-131.

[79] Yerokin A.L, X. Nie, A. Leyland, A. Matthews, S.J. Dowey. 1999. Plasma electrolysis for surface engineering. Surf Coat Tech;122: 73–93.

[80] Young, B., and J.W. Heath. 2000. Wheater's Functional Histology: a Text and Colour Atlas 4th Ed. Churchill Livingstone, UK.

[81] Zheng J. and G. Rawadi. 2003. BMP-2 Controls Alkaline Phosphatase Expression and Osteoblast Mineralization by a Wnt Autocrine Loop. Journal of Bone and Mineral Research, Volume 18, Number 10.pp 1842-1853.

A

pNPP Standard Curve

y = 0.2451x - 0.338
R² = 0.9788
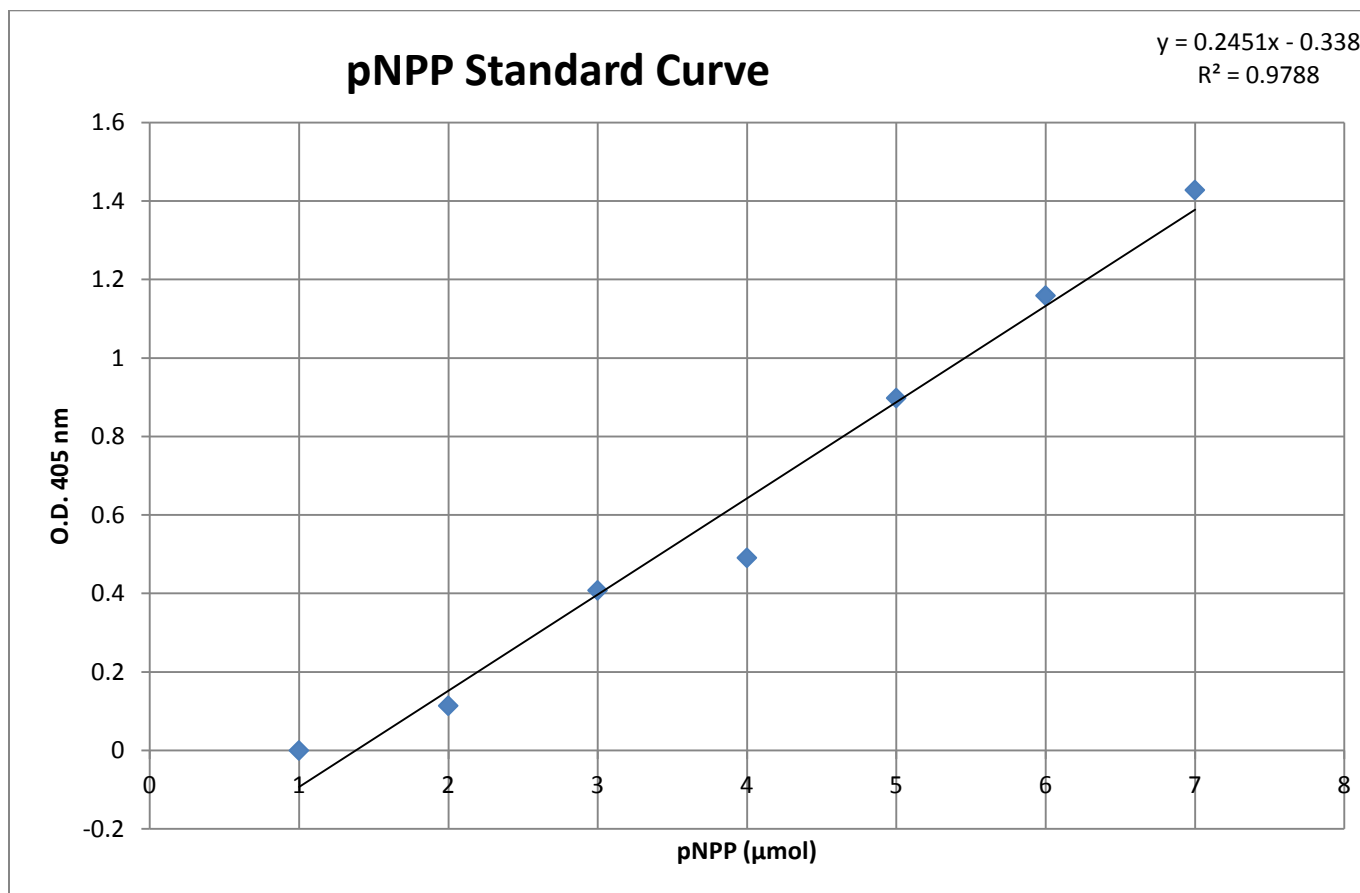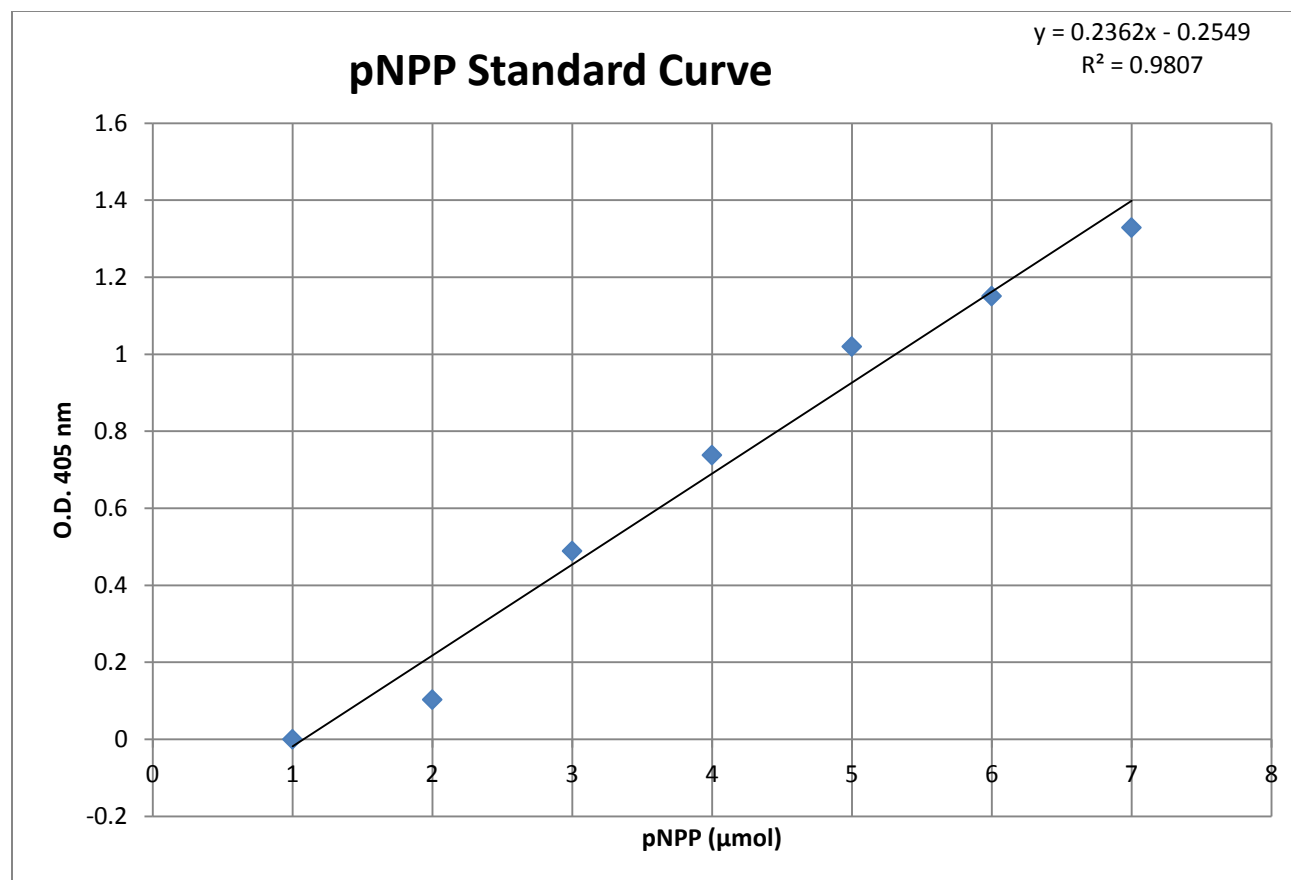
Figure 25: Standard Curves of absorbance at 405 nm versus pNPP produced by differentiated cells. The standard curves were performed to extrapolate the amount of pNPP produced. Standard curve A represents experiment 1and Standard curve B represents experiment 2. Absorbance was read at 405 nm. Data points reflect the mean ± standard deviation (S.D.) of the three repetitions per experiment.

Table 8: Estimated Optical Density and Alkaline Phosphatase Activity of Differentiated Cells on γ-TiAl and Ti-6Al-4V surfaces according to the type of metal (γ-TiAl and Ti-6Al-4V) and type of treatment (thermal or micro arc oxidation).

Type of metal	Treatment	Repetition	Optical Density	Alkaline phosphatase activity
Ti-6Al-4V	Coverslips	1	0.758667	0.0790280
Ti-6Al-4V	200mA, 3min.	1	0.854334	0.0889930
Ti-6Al-4V	200mA, 4min.	1	1.124334	0.1171180
Ti-6Al-4V	225mA, 3min.	1	1.161667	0.1210070
Ti-6Al-4V	225mA, 4min.	1	1.508334	0.1571180
Ti-6Al-4V	500°C	1	0.821674	0.0855910
Ti-6Al-4V	800°C	1	0.345000	0.0359380
Ti-6Al-4V	Negative control	1	0.012246	0.0012276
Ti-6Al-4V	Coverslips	2	0.723667	0.0753820
Ti-6Al-4V	200mA, 3min.	2	0.836333	0.0871180
Ti-6Al-4V	200mA, 4min.	2	1.016333	0.1058680
Ti-6Al-4V	225mA, 3min.	2	1.074999	0.1119790
Ti-6Al-4V	225mA, 4min.	2	1.218332	0.1269100
Ti-6Al-4V	500°C	2	0.817002	0.0851040
Ti-6Al-4V	800°C	2	0.106002	0.0110420

Ti-6Al-4V	Negative control	2	0.003086	0.0003210
Ti-6Al-4V	Coverslips	3	0.786333	0.0819100
Ti-6Al-4V	200mA, 3min.	3	0.893667	0.0930900
Ti-6Al-4V	200mA, 4min.	3	1.093667	0.1139240
Ti-6Al-4V	225mA, 3min.	3	1.139000	0.1186460
Ti-6Al-4V	225mA, 4min.	3	1.262333	0.1314930
Ti-6Al-4V	500°C	3	0.890000	0.0927080
Ti-6Al-4V	800°C	3	0.224000	0.0233330
Ti-6Al-4V	Negative control	3	0.002987	0.0003110
γ -TiAl	Coverslips	1	0.785333	0.0818060
γ - TiAl	200mA, 3min.	1	1.020333	0.1062850
γ - TiAl	200mA, 4min.	1	1.139666	0.1187150
γ - TiAl	225mA, 3min.	1	1.195000	0.1244790
γ - TiAl	225mA, 4min.	1	1.243000	0.1294790
γ - TiAl	500°C	1	0.903000	0.0940620
γ - TiAl	800°C	1	0.551999	0.0575000
γ - TiAl	Negative control	1	0.007647	0.0007970

γ - TiAl	Coverslips	2	0.921454	0.0959850
γ - TiAl	200mA, 3min.	2	1.199454	0.1249430
γ - TiAl	200mA, 4min.	2	1.319787	0.1374780
γ - TiAl	225mA, 3min.	2	1.387120	0.1444920
γ - TiAl	225mA, 4min.	2	1.437120	0.1497000
γ - TiAl	500°C	2	0.957120	0.0997000
γ - TiAl	800°C	2	0.570120	0.0593880
γ - TiAl	Negative control	2	0.002187	0.0002280
γ - TiAl	Coverslips	3	0.817667	0.0851740
γ - TiAl	200mA, 3min.	3	1.052667	0.1096530
γ - TiAl	200mA, 4min.	3	1.172000	0.1220830
γ - TiAl	225mA, 3min.	3	1.227333	0.1278470
γ - TiAl	225mA, 4min.	3	1.275333	0.1328470
γ - TiAl	500°C	3	0.935333	0.0974310
γ - TiAl	800°C	3	0.584333	0.0608680
γ - TiAl	Negative control	3	0.003293	0.0003430

APPENDIX B

1. ANOVA for Optical Density of Differentiated cells versus Metal (γ- TiAl and Ti-6Al-4V) and Type of Treatment (thermal and micro arc oxidation).

Analysis of variance

Variable	N	R²	Adj R²	CV	
Optical Density	48	0.98	0.97	9.32	

Analysis of variance table (Partial SS)

S.V.	SS	df	MS	F	p-value
Model.	8.56	17	0.50	81.83	<0.0001
Alloy	0.19	1	0.19	31.17	<0.0001
Treatment	8.22	7	1.17	190.88	<0.0001
Experiment	1.7E-03	2	8.7E-04	0.14	0.8693
Alloy*Treatment	0.15	7	0.02	3.37	0.0090
Error	0.18	30	0.01		
Total	8.75	47			

2. Fisher's LSD for Optical Density to compare the interaction between type of metal (γ TiAl, Ti-6Al-4V) and type of treatment (thermal and micro arc oxidation).

Test:Fisher LSD Alpha:=0.05 LSD:=0.13081
Error: 0.0062 df: 30

Alloy	Treatment	Means	n	S.E.								
γ-TiAl	Negative control	4.4E-03	3	0.05	A							
Ti-6Al-4V	Negative control	0.01	3	0.05	A							
Ti-6Al-4V	800	0.23	3	0.05		B						
γ-TiAl	800	0.57	3	0.05			C					
Ti-6Al-4V	Coverslips	0.76	3	0.05				D				
γ-TiAl	Coverslips	0.84	3	0.05				D	E			
Ti-6Al-4V	500	0.84	3	0.05				D	E			
Ti-6Al-4V	200mA+3min.	0.86	3	0.05				D	E			
γ-TiAl	500	0.93	3	0.05					E			
Ti-6Al-4V	200mA+4min.	1.08	3	0.05						F		
γ-TiAl	200mA+3min.	1.09	3	0.05						F	G	
Ti-6Al-4V	225mA+3min.	1.13	3	0.05						F	G	
γ-TiAl	200mA+4min.	1.21	3	0.05							G	H
γ-TiAl	225mA+3min.	1.27	3	0.05								H
γ-TiAl	225mA+4min.	1.32	3	0.05								H
Ti-6Al-4V	225mA+4min.	1.33	3	0.05								H

Means with a common letter are not significantly different (p<= 0.05)

1.**ANOVA for Alkaline Phosphatase activity of Differentiated cells versus Metal (γ-TiAl and Ti-6Al-4V) and Type of Treatment (thermal and micro arc oxidation).**

Variable	N	R²	Adj R²	CV
ALP	48	0.98	0.97	9.32

Analysis of variance table (Partial SS)

S.V.	SS	df	MS	F	p-value
Model.	0.09	17	0.01	81.84	<0.0001
Alloy	2.1E-03	1	2.1E-03	31.18	<0.0001
Treatment	0.09	7	0.01	190.90	<0.0001
Experiment	1.9E-05	2	9.4E-06	0.14	0.8692
Alloy*Treatment	1.6E-03	7	2.2E-04	3.37	0.0091
Error	2.0E-03	30	6.7E-05		
Total	0.09	47			

2. **Fisher's LSD for Alkaline Phosphatase activity to compare the interaction between type of metal (γ-TiAl, Ti-6Al-4V) and type of treatment (thermal and micro arc oxidation).**

**Test:Fisher LSD Alpha:=0.05 LSD:=0.01363**
Error: 0.0001 df: 30

Alloy	Treatment	Means	n	S.E.								
γ-TiAl	Negative control	4.6E-04	3	4.7E-03	A							
Ti-6Al-4V	Negative control	6.2E-04	3	4.7E-03	A							
Ti-6Al-4V	800	0.02	3	4.7E-03		B						
γ-TiAl	800	0.06	3	4.7E-03			C					
Ti-6Al-4V	Coverslips	0.08	3	4.7E-03				D				
γ-TiAl	Coverslips	0.09	3	4.7E-03				D	E			
Ti-6Al-4V	500	0.09	3	4.7E-03				D	E			
Ti-6Al-4V	200mA+3min.	0.09	3	4.7E-03				D	E			
γ-TiAl	500	0.10	3	4.7E-03					E			
Ti-6Al-4V	200mA+4min.	0.11	3	4.7E-03						F		
γ-TiAl	200mA+3min.	0.11	3	4.7E-03						F	G	
Ti-6Al-4V	225mA+3min.	0.12	3	4.7E-03						F	G	
γ-TiAl	200mA+4min.	0.13	3	4.7E-03							G	H
γ-TiAl	225mA+3min.	0.13	3	4.7E-03								H
γ-TiAl	225mA+4min.	0.14	3	4.7E-03								H
Ti-6Al-4V	225mA+4min.	0.14	3	4.7E-03								H

Means with a common letter are not significantly different (p<= 0.05)
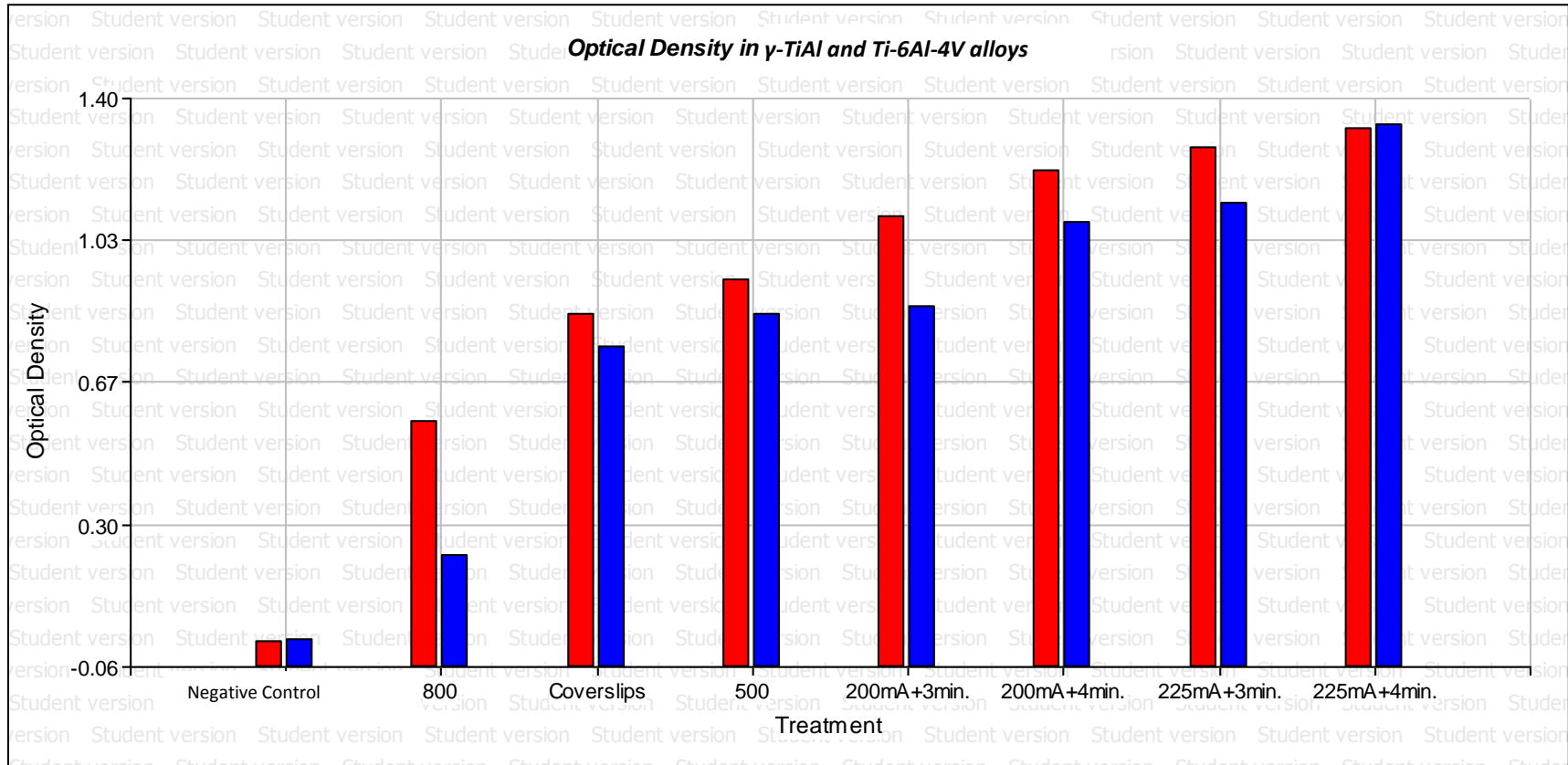
Figure 26: Optical Density in γ-TiAl and Ti-6Al-4V alloys.
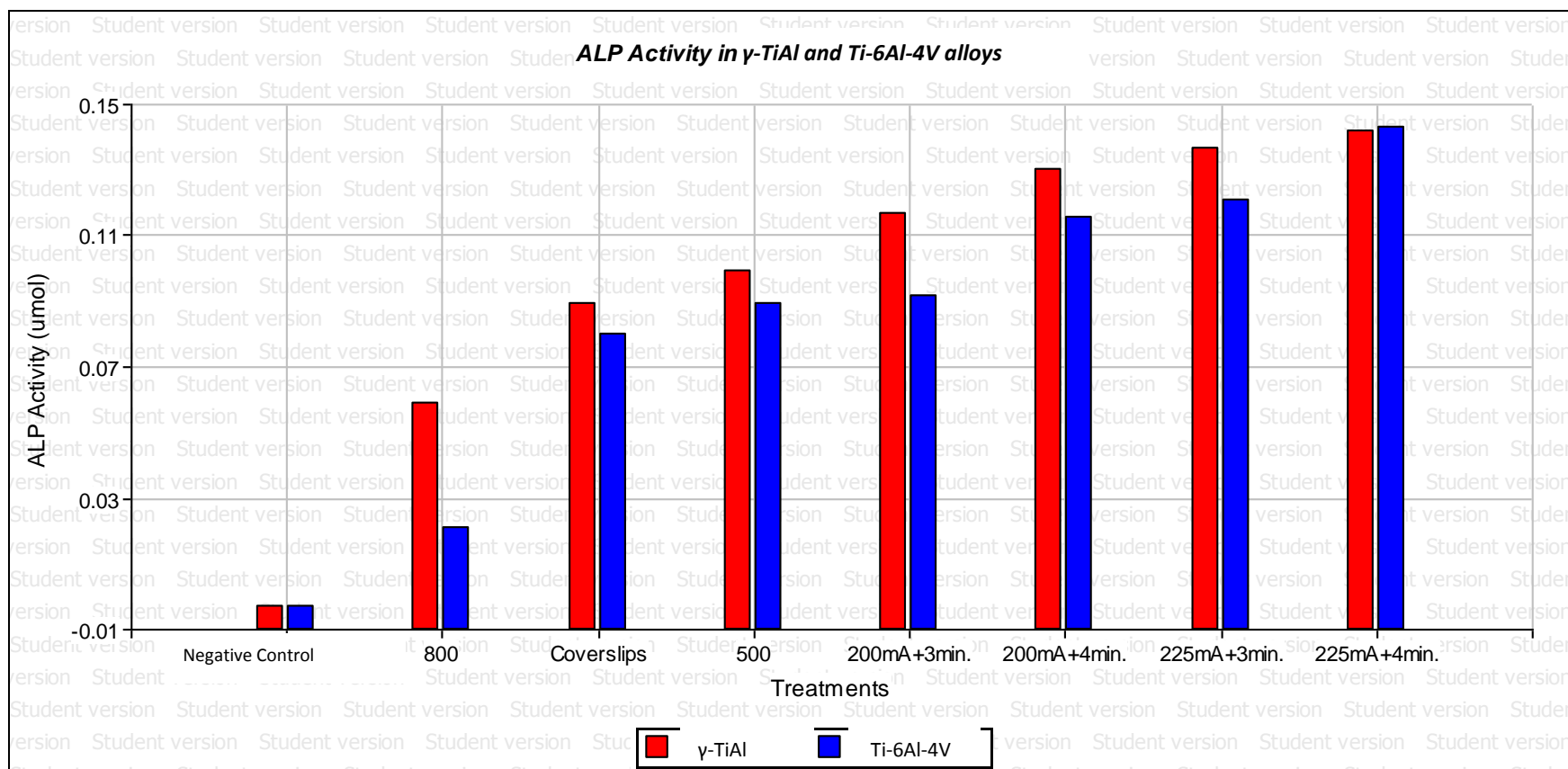
Figure 27: Alkaline phosphatase activity in γ-TiAl and Ti-6Al-4V alloys.